RSC Advances

REVIEW

View Article Online
View Journal | View Issue

Cite this: *RSC Adv.*, 2025, **15**, 27187

Advances in multimodal imaging techniques in nanomedicine: enhancing drug delivery precision

Vijay Mishra, [a] Neha Kumari,[a] Manish Vyas,[b] Alaa A. A. Aljabali, *[c] Aditi Chattaraj [d] and Yachana Mishra *[d]

Nanosystems that deliver drugs have revolutionized modern therapy *via* the accurate targeting and controlled release of drugs. The importance of real-time monitoring of these systems lies in the evaluation of their pharmacokinetics and biodistribution, as well as preventative treatment efficacy. Imaging methods thus gave birth to real-time monitoring, allowing visualization of nanoparticles (NPs) inside biological systems. This review introduces current imaging techniques such as optical imaging, computed tomography (CT), magnetic resonance imaging (MRI), nuclear imaging, ultrasound, and finally, hybrid techniques that are on the verge of being used. The principles, merits, demerits, and applications of each modality in tracking nanodrug delivery are summarized. Special importance is given to multimodal imaging based on the fact that it can help to overcome the limitations of any individual imaging modality, thereby offering better insight into drug delivery. Advances in imaging probes and imaging-guided drug delivery systems are illustrated to show this transformation of imaging in nanomedicine.

Received 9th May 2025
Accepted 27th June 2025

DOI: 10.1039/d5ra03255e

rsc.li/rsc-advances

Introduction

Nanodrug delivery has recently emerged as a revolutionary approach in contemporary medicine with the promise of enhancing therapeutic efficacy while minimizing side effects. Nanodrug delivery systems are nanoparticles (NPs) of sizes usually between 1 and 100 nm incorporated in therapeutics for the administration of drugs in specific tissues or to specific cells.[1] Nanodrug delivery systems enhance solubility and bioavailability, and provide controlled or sustained release technologies; hence, they are of tremendous importance for the treatment of very complicated diseases like cancer, neurodegenerative diseases, and even infectious diseases.[2] However, such advanced delivery systems require robust and precise monitoring techniques for optimization and validation. Imaging technologies are central and provide critical input toward understanding the biodistribution, pharmacokinetics, and therapeutic performance of nanodrug delivery systems. Advanced imaging modalities allow researchers to visualize the real-time journey of the NPs during *in vivo* studies, monitor their interactions with biological systems, and customize their designs for improved future clinical translations.[3]

[a]*School of Pharmaceutical Sciences, Lovely Professional University, Phagwara, Punjab-144411, India*

[b]*Research and Development Cell, Parul University, Vadodara, Gujarat-391760, India*

[c]*Department of Pharmaceutics & Pharmaceutical Technology, Yarmouk University, Irbid, Jordan. E-mail: alaaj@yu.edu.jo*

[d]*School of Bioengineering and Biosciences, Lovely Professional University, Phagwara, Punjab-144411, India. E-mail: yachanamishra@gmail.com*

Importance of nanodrug delivery

Nanodrug delivery systems have resulted in substantial progress within both pharmaceutical science and biomedical research. These systems reduce the various difficulties associated with traditional medication delivery systems. The use of conventional drug delivery methods leads to poor drug solubility and rapid removal from the body, as well as misdirected distribution, which can result in either insufficient therapeutic results or systemic safety issues.[4] NPs have distinct physicochemical properties that include a large size-to-volume ratio, along with adjustable size and adaptable surface modification. These entities simultaneously exhibit drug-containment capabilities, tissue-targeting functions, and biological-barrier-traversing properties. Stimuli-responsive components in nanodrug delivery systems release therapeutic agents based on recognized stimuli, including changes in pH levels, temperature fluctuations and activation of enzymatic activities. Nanodrug delivery systems attain high precision, which lowers the side effects of the drugs and strengthens their therapeutic power.[5] Researchers are actively examining nanodrug delivery systems based on their capacity to handle various drug delivery needs in areas including oncology as well as gene therapy and vaccine development. Government agencies rely on live tracking of nanodrug systems *via* imaging methods to determine their performance and behavior.[6]

Role of imaging techniques in drug delivery research

Field research of nanodrug delivery relies on indispensable imaging techniques that enable visual understanding and

analytical assessment of NPs inside biological systems. Scientists can evaluate biodistribution together with targeting efficiency and drug release kinetics with the help of these evaluation techniques.[7] Multiple advanced imaging approaches that include magnetic resonance imaging (MRI), optical coherence tomography (OCT), computed tomography (CT), fluorescence imaging, and positron emission tomography (PET) provide researchers with distinct capabilities to monitor NPs across multiple detection scales. MRI shows excellent capabilities for both high-resolution imaging and tissue differentiation, which enables researchers to track the distribution of magnetic NPs throughout the body. PET provides excellent detection sensitivity and allows quantification of the accumulation of radiolabeled probes within target tissues *via* its high sensitivity. The monitoring of NP cellular and molecular dynamics in real time is possible using fluorescent and bioluminescent optical imaging methods.[8]

Regarding the nanodrug delivery process, monitoring the implementation of multimodal imaging provides several benefits that merge unique capabilities from diverse modalities to yield complete observation insights. Researchers can enhance their knowledge of NP activities by uniting MRI with fluorescence imaging systems. Modern advances in imaging probe technologies, together with artificial intelligence (AI)-based image processing systems, now enable real-time non-invasive monitoring of nanodrug delivery systems. The detailed understanding of the interactions between NPs and biological systems provided by imaging techniques is required to enable the optimized design and functionality of nanodrug delivery systems and thus their successful clinical application.[9]

Overview of imaging techniques

Nanodrug delivery systems require imaging techniques for successful development and implementation (Fig. 1).[10] These investigative techniques reveal essential biological behavior together with the therapeutic performance of NPs, which enables researchers to develop improved designs for clinical purposes.[11] Various imaging techniques exist with different physical operation methods, ability to resolve details, and appropriate applications. Multiple factors such as sensitivity, spatial resolution, temporal resolution, and biocompatibility determine the choice of suitable imaging modalities. The following part presents the different categories of imaging modalities with an analysis of the essential factors needed to choose appropriate methods for nanodrug delivery research.[12]

Classification of imaging modalities

Research into nanodrug delivery utilizes three broad classes of imaging techniques, which include imaging of anatomical structures, functional assessment, and molecular investigations, with respective strengths and weaknesses. Anatomical imaging applications generally use MRI and CT, as they offer visualization of the structural components of the human body. The high spatial resolution and excellent soft tissue contrast of MRI make it suitable for monitoring NPs throughout complex biological surroundings. CT excels at visualizing hard tissues and acquires data immediately, which is beneficial for bone-targeted drug delivery applications.[13]

Functional imaging techniques such as PET and single-photon emission computed tomography (SPECT) have been developed to trace biological activities that occur inside living organisms. These techniques provide high sensitivity for tracking the movement of NPs throughout the body and

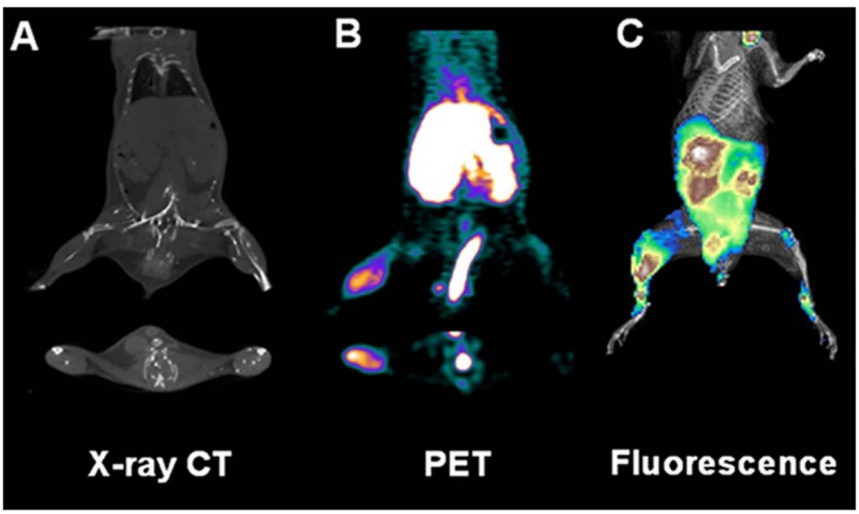

Fig. 1 Multimodal multifunctional nanoparticles allow the *in vivo* imaging of anatomy, physiology, and molecular events at various spatio-temporal scales.[10] Reproduced from ref. 10. Shown here are representative images of a mouse subjected to surgical ligation of the right femoral artery to induce hindlimb ischemia followed by the inflammatory response, which is assessed with a receptor for an advanced glycation end product (RAGE)-targeted nanoparticle-based multimodal agent labeled with both fluorophore (rhodamine) and radioisotope (^{64}Cu). The anatomy was assessed with X-ray computed tomography (CT) imaging (A). In contrast, molecular proinflammatory events were quantitatively assessed *in vivo* with positron emission tomographic (PET) imaging (B), whole-body fluorescence (C).

measuring their metabolism before elimination. Fluorescence and bioluminescence imaging provide molecular imaging methods to detect specific molecular communications between cells. The methods are specifically beneficial for tracking how NPs interact with cells at different levels and how treatments evolve in real time.[14]

The combination of different modalities through hybrid imaging systems, including PET/MRI and CT/SPECT, provides detailed knowledge about nanodrug delivery systems by harnessing the advantages of each technique. PET/MRI systems use the high sensitivity of PET and the high resolution of MRI to offer functional and anatomical imaging at the same time. Multimodal imaging probes have become significant because they unite different imaging agents into a single NP to generate complete information across several imaging platforms.[15]

The research objectives, together with the attributes of the studied nanodrug delivery systems, determine which specific imaging technique will be selected from among the available options based on each the different capabilities and weaknesses of each technique. The proper selection of modalities for imaging demands a thorough evaluation of their penetration capacity, resolution power and possibility for clinical usage.[16]

Criteria for selecting imaging techniques

During preclinical and clinical research, proper imaging techniques for nanodrug delivery systems are needed to guarantee success. Multiple essential factors should be evaluated to select an optimal imaging approach that suits the particular applications. The selection process depends heavily on five main image evaluation factors, which are sensitivity, spatial resolution, temporal resolution, biocompatibility, and cost-effectiveness.[17]

An imaging method should demonstrate high sensitivity by detecting minute amounts of NPs present in biological tissues. PET and fluorescence imaging, along with other high-sensitivity techniques, are typically used for the *in vivo* detection of low NP concentrations. The spatial resolution establishes the maximum level of anatomical detail that a visualization technique can display.[18] MRI and CT deliver precise spatial resolution, which enables developers to perform detailed structural imaging for their applications.[19]

The critical factors in research involving dynamic processes using NPs are both precise measurement of time duration as well as accurate timing of observations. Real-time fluorescence imaging is a technique that provides high temporal resolution to monitor NP movements over time continuously. Research techniques and imaging agents must match biological requirements, because their implementation may result in negative impacts on living organisms. For prolonged experimentation, non-invasive imaging approaches with low toxicity using MRI and bioluminescence imaging techniques constitute an optimal selection.[20]

Accessibility and budget significantly impact the decision-making process regarding imaging technologies. PET imaging agents and hybrid systems produce superior imaging results, but their vendor costs remain high and their availability is limited. Research institutions prefer optical imaging technologies because they offer both affordability and widespread availability that suit their preclinical needs.[21]

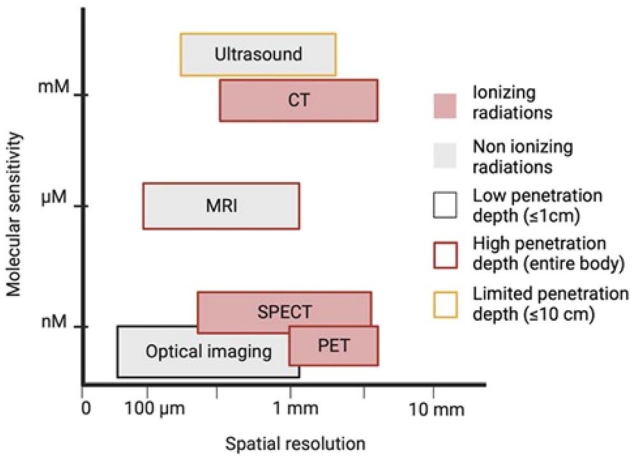

Fig. 2 Sensitivity and spatial resolution ranges of different imaging modalities.[23] Reproduced from ref. 23.

The integration of two recent technological advancements, AI and machine learning (ML), is now a central consideration in imaging data analysis. AI-driven approaches improve complicated image dataset interpretation and quantity precision, as well as automating workflows for image processing. The advanced analytical tools adopted by researchers enable imaging techniques to perform at their utmost level in nanodrug delivery research.[22]

Research success becomes achievable through deliberate evaluation of the criteria followed by a balanced assessment of the trade-offs between different imaging modalities, thus allowing scientists to choose research-specific imaging methods. Continuing advancements in imaging equipment, along with data processing capabilities, will lead to improved accuracy in nanodrug delivery research while facilitating the application of nanodrugs in medical practices (Fig. 2).[23]

Optical imaging

The visual capabilities of nanodrug delivery research depend heavily on optical imaging techniques, as these approaches deliver superior molecular details and superior sensitivity to biological systems. Light-based detection tools enable scientists to examine NPs while monitoring medicinal agents and studying tissue–NP relationships at different magnifications. Scientists organize optical imaging into three main categories, namely, fluorescence imaging, bioluminescence imaging, and near-infrared (NIR) imaging, which contribute different strengths to preclinical and clinical studies.

He *et al.* reported a NIR-II fluorophore based on DSPE-mPEG encapsulated rare earth doped NPs (RENPs@DSPE-mPEG), which showed inherent affinity toward bone without linking any targeting ligands, thus providing an alternative non-invasive, non-radiation-based strategy for skeletal system mapping and bone disease diagnosis. Interestingly, within the NIR-II window, imaging at a longer wavelength (1345 nm) provides a higher resolution and signal-to-noise ratio than imaging at 1064 nm,

even though the quantum yield at 1064 nm is two-fold higher than that at 1345 nm. In addition to bone imaging, RENPs@DSPE-mPEG shows imaging applications in blood vessels and lymph nodes. Importantly, RENPs@DSPE-mPEG can be internalized by circulating white blood cells (WBCs).[24]

Fluorescence imaging

Fluorescence imaging stands as the most prevalent optical detection approach used by researchers in nanodrug delivery investigations.[18] The use of fluorescent dyes and quantum dots in conjunction with NPs enables therapeutic agent labeling to display visible images under excitation light. The technique provides researchers with broad application capabilities that support the tracking of NPs inside cell cultures as well as within living subjects. Fluorescence imaging displays excellent spatial resolution capabilities that allow scientists to study cellular and subcellular processes. Fluorescence microscopy has shown its effectiveness in monitoring how NPs enter cells and following their cellular movement while also tracking therapeutic agent release through real-time observations.[25]

Impressive gains in fluorophore chemistry have enabled scientists to make dyes with enhanced brightness and stability while remaining biocompatible, thus improving the reliability and sensitivity of fluorescence imaging. The application of fluorescence imaging benefits nanodrug delivery assessment through identification of the efficiency of the targeting mechanisms.[16] NPs that receive targeting ligand modifications become responsive to fluorescent tags, which verify their specific accumulation in both tissue and cellular locations. This capability becomes essential for evaluating tumor-targeting strategies, as well as strategies related to precision medicine. Because of its inherent challenges, fluorescence imaging presents difficulties in detecting signals in the presence of tissue autofluorescence and shallow tissue penetration. Scientists have solved the current technical limitations by integrating fluorescence imaging with additional imaging methods, as well as by creating fluorophores able to operate under near-infrared wavelengths with enhanced tissue penetration capabilities.[17]

Observing the release and activation of prodrug formulations provides essential data concerning therapy efficacy. While several imaging modalities can be employed to assess prodrug delivery, confirming the release of the active payload through imaging presents challenges. Uyar *et al.* demonstrated that the switchable fluorescence of doxorubicin (DOX) can validate drug release after an uncaging reaction with a highly selective chemical counterpart. The conjugation of DOX with *trans*-cyclooctene (TCO) diminishes its fluorescence at 595 nm. The quenched fluorescence of the DOX prodrug is restored during the bond-cleaving reaction with tetrazine. The switchable fluorescence mechanism of DOX may be utilized for fundamental studies, including the reactivity of different tetrazine and TCO linker types under diverse experimental conditions.[26]

Bioluminescence imaging

The optical imaging technique known as bioluminescence imaging (BLI) enables scientists to detect light that emanates from enzymatic chemical reactions inside living creatures. BLI generates emission without external light sources, thus resulting in low background interference and strong signal quality. The ability of bioluminescence imaging to generate light from the host enables its use in *in vivo* studies, especially in preclinical research. Scientists use BLI extensively as an investigative tool to track NPs throughout animal models to study their movement, along with their pharmacokinetic attributes and therapeutic functions. The monitoring of luciferase-enzyme-conjugated NP distribution in target mouse tissues can be conducted noninvasively. The longitudinal observation of nanodrug delivery systems becomes possible through this method, which prevents animal sacrifices during prolonged research periods. Bioluminescence imaging demonstrates exceptional sensitivity because it allows scientists to detect small quantities of NPs.[17]

Ruiz del Rio *et al.* created fluorescent extracellular vesicles (EVs) and a bioluminescent nanodrug to study their accumulation in fibrotic hearts and lungs. The biodistribution of the medication in several organs was determined by detecting Au in the drug nanostructure. They discovered that nanodrug-containing EVs can reach fibrotic hearts and lungs *in vivo*, improving free drug biodistribution.[10,27]

Magnetic resonance imaging

MRI is one of the most advanced and adjustable imaging systems utilized by researchers for studying nanodrug delivery. This technology delivers superior spatial imaging quality, and the integrated algorithm provides exceptional tissue distinction along with real-time detection of biological processes. The tracking of NPs combined with biological system interactions becomes more effective through MRI, because it offers both non-invasive procedures and long-term monitoring capability. The field of nanodrug delivery has used MRI techniques to determine the biodistribution of drugs and measure drug kinetics to evaluate drug effectiveness.[19]

Surasinghe *et al.* developed a targeted uSPIO-5D3-DM1-AF488/CF750 nanotheranostic modality for the treatment of PSMA(+) prostate cancer. The researchers used ultrasmall superparamagnetic iron oxide (uSPIO) NPs conjugated with 5D3 monoclonal antibody, an anti-prostate-specific membrane antigen (PSMA), the anti-tubulin agent mertansine (DM1), and a fluorophore (AF488/CF750). The developed formulation facilitates multimodal *in vivo* imaging utilizing NIR fluorescence and MRI.[28]

Halim *et al.* used magnetic iron oxide NPs as a delivery platform to facilitate the transport of active antisense oligonucleotides to tumors. These NPs are engineered to target tissues exhibiting enhanced vascular permeability, especially those impacted by inflammation or malignancy. The magnetic properties of these NPs enable their *in vivo* tracking using MRI. This therapeutic approach aligns with this important imaging technology, facilitating its clinical translation. They can also be labeled with diverse imaging reporters, including a Cy5.5 NIR optical dye for correlational optical imaging and fluorescence microscopy.[29]

Principles of MRI

The operating principle of MRI is nuclear magnetic resonance (NMR), in which atomic nuclei react to magnetic fields. The magnetic field affects specific atomic nuclei such as protons in hydrogen, which demonstrate magnetic alignment because of their spin-based properties. When placed under the influence of a powerful external magnetic field, these nuclei produce a total magnetism from their two possible alignments. The introduction of radiofrequency (RF) pulses interrupts this alignment between atomic nuclei and magnetic fields, thus causing their energy to be absorbed and rise to a higher state. Detection equipment processes the emitted RF signals to create precise images of different tissues. The contrast in MRI images depends primarily on the relaxation times of the tissues, tracking how fast the protons recover from an excitation event.[12,13] The relaxation mechanisms of MRI consist mainly of two processes, which are T1 relaxation and T2 relaxation. The basic contrast seen in MRI scans originates from the different relaxation time variations between different tissues. Medical imaging benefits from this tissue differentiation ability to depict NPs and their biological environment distribution patterns. The versatile nature of MRI results from its ability to perform three-dimensional (3D) imaging, together with its capability to work with exogenous contrast agents. Repeated use of MRI is safe because it lacks the ionizing radiation components found in CT while offering excellent suitability for time-dependent nanodrug delivery system assessment during extended research periods.[29]

Contrast agents for nanoparticle detection

The detection capabilities of MRI for NPs are improved through the use of contrast agents. The agents modify the proton relaxation properties of surrounding water molecules to enhance tissue structure detection. The two main categories of MRI contrast agents are those that generate positive T1 contrast effects and those that produce negative T2 contrast effects.[30]

T1 agents (positive contrast). The administration of T1 agents leads to the shortening of water proton T1 relaxation times, which produces brighter signals in MRI images. Gadolinium-based contrast agents (GBCAs) are the primary T1 agents because they demonstrate powerful paramagnetic characteristics. The intensified signals from MRI make these agents useful for identifying blood vessels, tumors and well-perfused organs by detecting NP accumulations in the tissue. Researchers have developed NPs that integrate gadolinium (Gd) so that they become visible under MRI procedures by applying the material as either a surface coating or central element.[31]

T2 agents (negative contrast). The T2 relaxation period of water protons is shortened by T2 agents, which results in diminished signal intensity that creates darker areas when MRI is used to produce images. Because of their high magnetic susceptibility and biocompatibility, SPIONs find extensive use as T2 agents. SPIONs have undergone extensive research for cancer imaging to achieve both detection of tumors and tracking of the biodistribution of therapeutic NPs.[13]

Scientists have developed NP-based therapeutic and imaging contrast agents that combine diagnosis with treatment through the therapeutic nanotechnology known as theranostics. Drug delivery systems consisting of NPs can contain both therapeutic loads and target-specific ligand compounds and tracking elements, allowing medical professionals to achieve real-time drug delivery monitoring and treatment evaluation. Scientific teams have developed SPIONs containing chemotherapeutic drugs attached to targeting molecules for precise tumor targeting, while MRI provides real-time treatment observation.[32]

Zhang *et al.* ingeniously coupled the antibody profilin-1 (PFN1), which actively targets vascular smooth muscle cells, with SPIONs, and subsequently incorporated rapamycin and Cy5.5. This innovative approach resulted in the development of dual-mode imaging NPs with therapeutic potential against atherosclerotic plaques. The study demonstrated that these NPs could effectively locate atherosclerotic plaques through passive penetration and specific targeting of vascular smooth muscle cells in ApoE−/− mice, which were observable through NIRF and *in vivo* MRI.[33]

In another study, IONPs and rapamycin were encapsulated within liposomes and further modified with a fluorescent reagent. These NPs were ingeniously equipped with the targeting peptide VHPKQHR (VHP) to enable specific recognition and binding to VCAM-1 on endothelial cells. The results demonstrated the efficacy of the synthesized theranostic as an excellent label for bimodal MRI and fluorescence imaging of atherosclerosis, showcasing its promising potential for early diagnosis.[34]

Zhang *et al.* synthesized uSPIO of approximately 3 nm *via* high-temperature thermal decomposition. Subsequent surface modification facilitated the development of a dual-modality magnetic resonance/fluorescence probe. Upon intravenous administration of the probes, an MRI assessment of atherosclerotic plaques and diagnostic evaluation were conducted. The application of Flash-3D sequence imaging revealed vascular constriction at lesion sites, accompanied by a gradual signal amplification after probe injection. T1-weighted imaging of the carotid artery unveiled a progressive signal ratio increase between plaques and controls within 72 h post-administration. Fluorescence imaging of isolated carotid arteries exhibited incremental lesion-to-control signal ratios. Additionally, T1 imaging of the aorta demonstrated an evolving signal enhancement over 48 h. Therefore, the uSPIO holds immense promise for the early and non-invasive diagnosis of plaques, providing an avenue for dynamic evaluation over an extended time frame.[35]

The advantages of using NPs as contrast agents include extended circulation duration, targeted delivery capability, and the ability to penetrate biological barriers. The safety and effectiveness of NPs has also been improved through innovative methods of synthesis that utilize biodegradable polymers along with lipid coatings.[13]

One recent work effectively illustrates the capability of identifying NPs with MRI/MRS properties without probe functionalization utilizing ^{1}H CSI. Among the nanosystems studied, the perfluorocarbon-based nanoemulsion had the greatest SNR. As a result, it was tested *in vivo*, and could be detected within

tumors and inflamed areas using ^{1}H CSI and in lymph nodes *via* PRESS.[32]

Ultra-high-field (UHF) MRI provides substantial advantages compared to low-field MRI. Although gadolinium chelates are the most often utilized MRI contrast agents, their efficacy diminishes under high magnetic fields, leading to significantly decreased T1 intensity. Holmium (Ho)-based NPs have significant potential as T2-weighted MRI contrast agents in ultra-high-frequency MRI, which is attributed to their remarkably low electron relaxation times (about 10–13 s). In one study, a multifunctional nanotherapeutic probe was developed for UHF MRI-guided chemotherapy and photothermal therapy (PTT). The chemotherapeutic agent mitoxantrone (MTO) was encapsulated into Ho(III)-doped mesoporous polydopamine (Ho-MPDA, HM) nanospheres, which were then coated with 4T1 cell membranes to enhance targeted delivery to breast cancer. The results indicated the potential of a distinctive UHF MRI-guided multifunctional nanosystem in cancer treatment.[36]

Functional MRI in nanodrug delivery

MRI technology has been expanded through functional MRI (fMRI), which provides the ability to monitor biological and chemical processes. This sophisticated imaging method is an essential nanodrug delivery research instrument that shows researchers how therapeutic actions affect living systems and how NPs move within organisms.[37]

Since 1992, the blood-oxygen-level-dependent (BOLD) fMRI technique has been the most widely used *in vivo* imaging method for functional brain imaging. BOLD fMRI delivers functional information without the need for intrusive electrodes, radiation, or an intravenous contrast agent. The BOLD fMRI signal depends on cerebral blood flow, volume, and metabolic rate.[9] The non-invasive dynamic contrast-enhanced MRI (DCE-MRI) approach gives useful information on tissue perfusion and vascularity. DCE-MRI is commonly employed in cancer to evaluate morphology and contrast agent (CA) kinetics in the tissue of interest. The temporal fingerprints of DCE-MRI data are interpreted using quantitative, semi-quantitative, and qualitative methodologies.[38] Diffusion-weighted imaging (DWI) is a non-contrast MRI method used to study the diffusion of water molecules inside biological tissues. Numerous studies have shown that multiparametric MRI (mpMRI), combining DWI and DCE MRI, enhances the specificity and diagnostic accuracy of breast lesion characterization, thus minimizing needless biopsies of benign lesions.[39]

A study using fMRI was conducted to detect hemodynamic and microenvironmental alterations in a lung cancer xenograft model that was administered DOX contained inside a cyclic arginine-glycine-aspartic acid polypeptide modified poly(lactic-*co*-glycolic acid) nanosystem (cRGD-PLGA@DOX). Two functional MRI approaches, IVIM-DWI and R2* mapping, can detect changes in the tumor microenvironment (TME) during treatment without necessitating invasive procedures.[40,41]

Biocompatible hyaluronic acid (HA)-guided cerasomes were generated to selectively target CD44-positive cells within the plaque during *in vitro* studies and *in vivo* testing in ApoE−/− mice. Rosuvastatin (RST) was encapsulated in the HA-guided cerasome nano-formulation to produce HA-CC-RST, which results in significant plaque regression as compared to treatment with the free drug. Gadodiamide-loaded HA-CC enhances MRI of vulnerable plaques, thereby attaining the goal of improved simultaneous treatment and imaging. Transcriptomic analysis confirmed plaque regression with HA-CC-RST treatment, which potentially benefitted from the anti-inflammatory effect of RST.[42]

Cao *et al.* used diffusion-weighted and BOLD MRI following nanographene oxide-mediated PTT and photodynamic therapy (PDT). The authors indicated that effective PTT leads to a significant elevation in the tumor apparent diffusion coefficient (ADC) value in DWI maps, whereas effective PDT results in an enhancement in BOLD images. In all scenarios, the extent of the increase correlated with treatment outcomes. Synergistic therapeutic efficacy was shown with the administration of the PTT/PDT combination, which was associated with a greater ADC and enhancement compared to the use of either modality in isolation. These results demonstrate the significant potential of combining DWI and BOLD MRI as tools for precise monitoring and prognosis of phototherapies. This is significantly important for the future development of these procedures.[43] The underlying principle of the DWI technique is represented in Fig. 3.[44]

Computed tomography

Mechanisms and applications. CT imaging relies on X-ray technology to build cross-sectional pictures of body structures, including tissues and organs, through its scan process. Medical image practitioners use this technology extensively because it provides comprehensive 3D anatomical details with high resolution. The imaging procedure of CT scans involves transmitting X-rays into the body from different directions to create images using detector receptacles. The signals recorded by the detectors enter a computer system, where algorithms transform them into precise photographic slices that show the complete area of interest. CT remains fundamental within nanodrug delivery research for observing how NPs distribute within the body, specifically in difficult-to-image areas such as bones and lungs.[45]

CT imaging can detect calcium phosphate NPs delivered for bone therapy, as these particles have strong X-ray attenuation capabilities. CT has proven effective in monitoring the distribution characteristics of NPs intended to treat lung conditions in medical research. CT excels due to its ability to produce highly detailed anatomical studies because of its superior spatial resolution. The exact localization of NPs becomes possible when using this technology in both preclinical research and clinical medical practice. However, CT imaging has several constraints that prevent the system from delivering functional or molecular information about subjects. Researchers have studied the combination of CT imaging with PET or MRI technologies to create multimodal imaging systems that tackle this limitation.[46]

Nanodrug delivery devices with multimodal imaging capabilities are worth investigating because they combine diagnostic

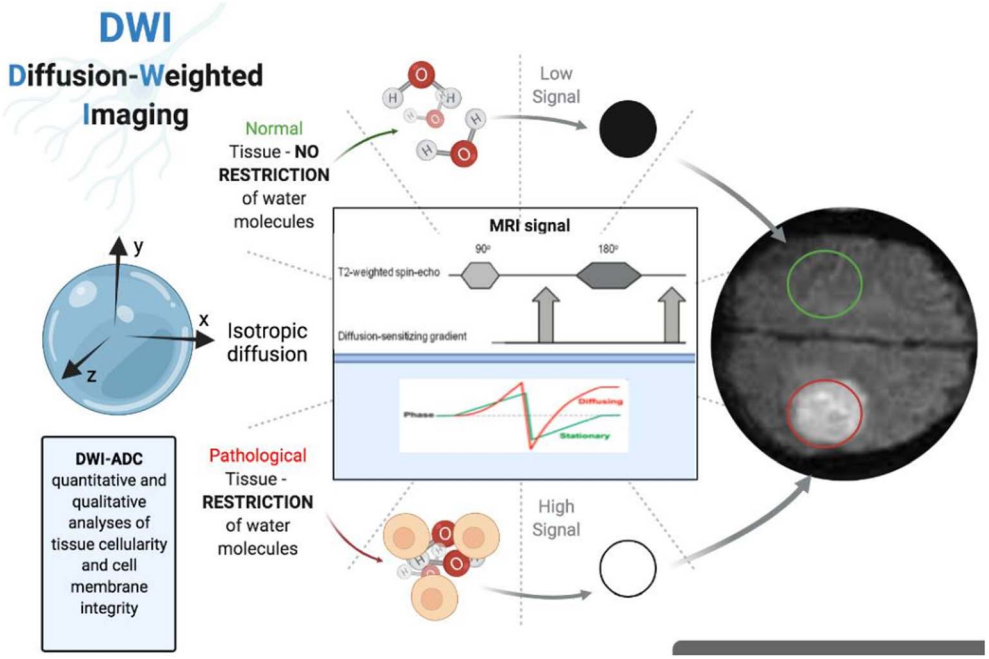

Fig. 3 Physical principles of diffusion-weighted imaging (DWI).[44] Reproduced from ref. 44.

and therapeutic activities. Zhang *et al.* designed and developed modified iridium sulfide (IrSx) NPs, which were tested *in vitro* and *in vivo* for cancer treatment. CT imaging provided a useful method for monitoring the therapy effects.[47]

Naha *et al.* developed a CT contrast agent, *i.e.*, dextran-coated cerium oxide NPs (Dex-CeNP) for gastrointestinal tract (GIT) imaging of inflammatory bowel disease (IBD). The CT contrast generation and accumulation of the Dex-CeNP at inflammation sites were compared with those of iopamidol, an FDA-approved CT contrast agent. Dex-CeNP was found to be protective against oxidative damage. Dex-CeNP produced strong CT contrast and accumulated in the colitis area of the large intestine. Therefore, Dex-CeNP can be used as a potential CT contrast agent for imaging GIT with IBD while protecting against oxidative damage.[48]

Nanoparticle-based contrast agents. CT imaging sensitivity requires enhancement using contrast agents so that medical staff can track NPs. These agents enhance tissue visualization by attracting X-rays more strongly than adjacent anatomical areas. Radiological scientists have developed NP-based agents as CT imaging contrast agents that offer improved targeting and enhanced specificity. Gold NPs (AuNPs) have proven to be optimal CT contrast agents, as they show high X-ray attenuation capability along with excellent biocompatibility.[49]

The NPs maintain specific targeting ligands, enabling their accumulation inside particular tissues, including tumors, to achieve precise imaging of diseased regions. Research has investigated the ability of AuNPs to perform theranostics by combining imaging and therapeutic functions in unified platforms. Iodine-based NPs show great potential as a second promising nanotechnology-based CT contrast agent option. These agents create an effective contrast between tissue regions, and medical professionals utilize them to obtain detailed images of tumors alongside blood vessels and anatomical structures. Advanced methods of NP synthesis have resulted in the creation of biodegradable iodine NPs that both lower the potential for toxic effects and enhance integration in medical applications. The development of hybrid NPs integrates various diagnostic and therapeutic features for CT imaging purposes.[50]

Photon-counting detectors (PCDs) represent an advanced technology that enables spectrum CT imaging in a single scan. Spectral imaging is extremely beneficial in contrast-enhanced CT (CECT) imaging, particularly when many contrast agents are employed, as the materials can be differentiated by their unique X-ray absorption characteristics. CECT has applications in joint imaging, which examines the structure and composition of articular cartilage soft tissue. A photon-counting detector CT (PCD-CT) approach paired with a dual-contrast agent method is used to assess articular cartilage and identify compositional alterations associated with early-stage osteoarthritis (OA). A mixture of proteoglycan-binding cationic tantalum oxide NPs and a commercial non-ionic iodinated iodixanol agent was utilized to perform the contrast. By evaluating the concentrations of the contrast agents, the approach allowed for a simultaneous assessment of the cartilage solid components and function. Within 12 h, the contrast agent diffusion differed considerably between the healthy and early-stage OA groups, depending on the contrast agent composition.[51]

Another study sought to assess iodinated NPs based on Visipaque for the identification of macrophages in atherosclerotic plaques using CT. *In vivo* CT imaging revealed that the density of NPs in aortic wall plaques was greater in atherosclerotic rabbits than in control rabbits. The authors concluded

that the new NPs may be a potential effective contrast agent for the identification of macrophages in atherosclerotic plaques utilizing CT.[52]

Despite the fact that both CT and MRI are widely recognized for their high-resolution imaging capabilities, their practical distinctions become particularly important when studying NP-based drug delivery systems. These discrepancies are mostly because of variances in their sensitivity to nanoscale probes, contrast mechanisms, and spatial resolution, all of which affect how well they work in both clinical and experimental settings. Because of its superior contrast and ability to provide precise spatial resolution—typically between 25 and 100 μm in sophisticated preclinical systems and around 0.5 and 1 mm in traditional clinical settings—MRI is especially useful for imaging soft tissues. MRI is a very useful tool for tracking the distribution of magnetic or paramagnetic NPs, such as gadolinium-based medicines or SPIONs, within biological tissues because of its high resolution and non-invasive nature. However, because the signal is averaged over very large voxel sizes, one of the main drawbacks of MRI in this situation is its inability to identify individual NPs. Therefore, to produce detectable contrast in tissues, substantial quantities of NPs, typically in the micromolar to millimolar range, are required.[53]

In contrast, CT provides better spatial resolution; current clinical CT scanners may achieve 250–500 μm, while micro-CT systems can reach about 50 μm. Because of this, CT is especially useful for imaging mineralized, high-density tissues like bone tissue. Effective imaging, however, frequently necessitates the use of particles containing high-atomic-number elements, such as gold or bismuth, which give greater X-ray attenuation, due to the restricted soft tissue contrast and poorer sensitivity of CT to typical NP compositions. CT is often less appropriate for dynamic, low-dose, or soft-tissue-focused imaging due to these constraints unless it is combined with contrast-enhancing agents or integrated into hybrid systems, such as CT-MRI combinations.[34,49]

The selection and design of research utilizing nanomedicine are greatly influenced by these differences in imaging capabilities. For soft tissue applications, such as tracking the NP activity in tumors or inflammatory cardiovascular tissues, MRI is typically preferred since it allows for long-term surveillance. On the other hand, CT is more frequently employed for mapping the biodistribution of NPs in calcified tissues, assessing bone-targeted nanocarriers, and conducting high-resolution anatomical evaluations. However, it is crucial to understand that individual NPs and their intracellular routes cannot be seen by MRI or CT. Higher-resolution methods like fluorescence imaging or super-resolution microscopy (SRM), which enable precise monitoring at the cellular and subcellular levels, are frequently used by researchers in conjunction with MRI and CT for these reasons.

There are still several obstacles that need to be overcome before NP-based contrast agents reach their optimal performance level for CT imaging. Clinical applications of NP agents require research to solve the problems that stem from NP aggregation, along with clearance issues and ensuring long-term biocompatibility. Research into nanodrug delivery with CT imaging will benefit from the development of new and improved contrast agents.

Nuclear imaging

Positron emission tomography. PET delivers highly sensitive nuclear imaging techniques to measure the quantitative biodistribution and pharmacokinetics of NPs inside living organisms. SPECT offers researchers excellent capability to examine the spatial distribution, along with the targeting effectiveness of NPs. One can detect gamma rays from positron-emitting radionuclides through PET imaging after inserting these radionuclides into NPs or drugs to view them. The high sensitivity of PET makes it essential for tracking nanodrug delivery systems, as it can detect trace amounts of radiolabeled NPs.[14]

The real-time whole-body imaging capability of PET makes it suitable for detecting NP biodistribution throughout different parts of the body during specific periods. Scientists have employed PET to monitor NPs, which bind to receptors displayed by particular tissues using ligand attachments. Researchers have employed fluorine-18 (^{18}F), a common radionuclide in PET, for NP labeling, which enabled visualization of therapeutic agent retention in tumor tissues. Carlson *et al.* created [^{18}F]OP-801 by radiolabeling a new hydroxyl dendrimer that is selectively taken up by reactive macrophages/microglia and tested its capacity to detect innate immunological activation in mice after a lipopolysaccharide (LPS) exposure. Gamma counting supported the PET data, revealing a considerably higher signal in the same regions compared to saline-injected animals. Brain PET/CT images (averaged 50–60 min) demonstrated a linear increase in [^{18}F]OP-801 uptake throughout the brain, which was substantially linked with murine sepsis scores. LPS-treated mice showed considerably greater tracer absorption in the brain stem, cortex, olfactory bulb, white matter, and ventricles than saline-treated animals. [^{18}F]OP-801 is a potential new PET tracer for the sensitive and selective detection of activated macrophages and microglia, necessitating more investigation.[54]

In recent research, Chen and coworkers developed ^{68}Ga-labeled amphiphilic alternating copolymer NPs with diverse rigid ligands as PET probes for imaging lymph node metastases. *In vivo* lymph node metastasis imaging revealed that PU (^{68}Ga-L-MDI-PEG) NPs exhibited significant accumulation in normal lymph nodes (N-LN) and tumor-metastasized sentinel lymph nodes (T-SLN), leading to divergent PET signal profiles, hence facilitating the differentiation between N-LN and T-SLN.[55]

PET imaging has the disadvantage of limited resolution and the need to account for molecular biodistribution, but it offers the benefit of great targeting precision. Methodological breakthroughs in radiochemistry, paired with stable radionuclide production, allow for improved uses of PET in nanodrug delivery studies.[56]

Single photon emission computed tomography. SPECT provides 3D distribution data for radiolabeled NPs through its imaging process. SPECT distinguishes itself from PET in detecting gamma rays from radionuclides directly, while PET uses positron detection. The SPECT technique utilizes two

commonly employed radionuclides, namely, technetium-99m (^{99m}Tc) and iodine-123 (^{123}I), which match adequately with the imaging time requirements. SPECT offers researchers an excellent capability to examine the spatial distribution and targeting effectiveness of NPs.[57]

The process of attaching targeting ligands and radiolabels to NPs enables researchers to observe tissue accumulation, particularly in tumors, along with inflammatory areas. Scientists utilize SPECT imaging systems to evaluate NPs intended for blood–brain barrier penetration because they offer essential information about particle delivery to brain target areas. The key benefit of the SPECT technique is its dual capability to examine various radionuclides in parallel, which facilitates the investigation of interconnected biological reactions.[58] The assessment of therapeutic and diagnostic isotope overlap has utilized two-isotope SPECT methods.[15]

In one study, thrombus formation was induced in C57Bl/6 mice by endothelial damage ($FeCl_3$) or ligation (stenosis) of the infrarenal *vena cava* (IVC). Dickhout *et al.* improved and validated the imaging probe using ^{111}In SPECT/CT in a mouse thrombosis model. In the stenosis model, clot formation in the *vena cava* corresponded with a SPECT hotspot using an A16 imaging probe as a molecular tracer. The fibrin-targeting A16 probe showed specific binding to mouse thrombi in *in vitro* assays and in an *in vivo* model. The use of specific and covalent fibrin-binding probes might enable the non-invasive clinical imaging of early and active thrombosis.[59]

Radiolabeling strategies for nanoparticles. The tracking and visualization of NPs inside biological systems requires the essential method of radiolabeling, which is utilized in nuclear imaging (Fig. 4).[60] Accurate biodistribution assessment and pharmacokinetics monitoring of NPs becomes possible when researchers introduce radioactive isotopes into their structure. Imaging systems support the extensive use of the radionuclides ^{18}F and ^{99m}Tc because of their optimal half-lives.[61]

Generally, direct radiolabelling of NPs is achieved by binding radioisotopes to the surface or encapsulating them in the core of NPs, while in indirect labeling, a chelator bridges the NP with the isotope. Acyclic or linear chelators include diethylenetriamine-*N*,*N*,*N*′,*N*,*N*-pentaacetic acid, pentetic acid, nitrilotriacetic acid (NTA), deferoxamine (DFO), and ((carboxymethyl) imino)bis(ethylenenitrilo)-tetra-acetic acid (DTPA). Examples of macrocyclic chelators are 2,2′,2″,2‴-(1,4,7,10-tetraazacyclododecane-1,4,7,10-tetrayl) tetraacetic acid (DOTA), 1,4,7-triazacyclononane-*N*,*N*′,*N*″-triacetic acid (NOTA), triethylenetetramine (TETA), 1,4,7-triazacyclononane, and 1-glutaric-4,7-acetic acid (NODAGA). Positron-emitting radionuclides generally have shorter half-lives compared to single-photon emitters. Carbon-11, nitrogen-13, oxygen-15, fluorine-18, and gallium-68 are the most often utilized radionuclides with short half-lives, ranging from 122 s to 109.7 min. The longer-lived positron emitters have half-lives of 12.701 h for copper-64, 78.4 h for zirconium-89, and 100.22 h for iodine-124. In indirect labeling, the most often utilized chelators are DOTA and NOTA.[62]

Ultrasound imaging

Basics of ultrasound imaging. High-frequency soundwaves are used in (US) to develop non-invasive images of body structures through a method known as ultrasound US imaging, which is frequently used by medical professionals. High-frequency soundwave signals enter the tissue through a transducer and then interact with biological structures inside the tissue. The soundwaves encounter interfaces between different tissues with dissimilar acoustic characteristics that result in their reflection back to the transducer, which uses the echoes to create electrical signals that are processed into real-time images. US imaging achieves its essential value through enabling real-time biological process observation, which makes it essential for both diagnostic purposes and therapy assessments. The visualization abilities of US prove most effective for detecting soft tissues and organs, including the heart, liver, and kidneys, which make it crucial for obstetrics, oncology care and cardiology evaluation. The absence of ionizing radiation makes

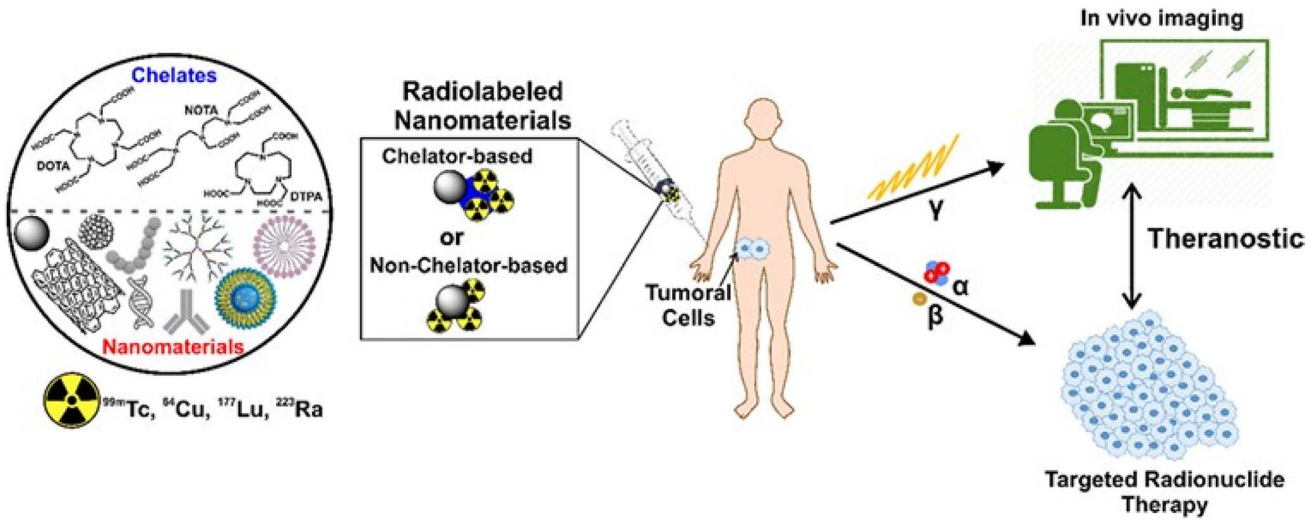

Fig. 4 Radiolabelled nanomaterials for biomedical applications.[60] Reproduced from ref. 60.

US a suitable diagnostic tool for multiple uses during both clinical patient care and preclinical evaluations.[60,63]

The use of US for visualizing nanodrug behaviors has become prevalent in research involving *in vivo* examinations of NPs. Research teams can monitor the real-time accumulation patterns of particles by analyzing high-definition images of both tissues and vascular structures. Scientists employ soundwave frequency control for imaging purposes, which enables examinations of target tissues at multiple depths and resolutions to study NP interaction patterns.[64]

Advancements in US imaging techniques have led to the development of two powerful methods: doppler US to measure blood flow velocity, and elastography to evaluate tissue stiffness. These tracking methods supply additional functional information that complement NP monitoring, especially in cancer diagnosis, since tissue rigidity and vascularization changes serve as crucial disease indicators.[65] The advantages in US imagery are limited by its inability to see through bone or air-filled cavities, and it provides lower resolution compared to MRI and CT devices. Ongoing developments in transducer engineering, along with image processing technique enhancements and contrast agent creation methods, continue to expand its operational abilities.[66] US imaging represents an essential research tool for nanodrug delivery because it combines safe technology with cost-effectiveness and time-sensitive operation capabilities (Fig. 5).[67]

Olsson *et al.* used an US image-guided method to improve treatment results during interstitial photothermal therapy (I-PTT), an investigational cancer treatment technique.[68] The effect of US-guided I-PTT (US I-PTT) on an aggressive pediatric solid tumor, neuroblastoma, was investigated using the 9464D syngeneic model in C57BL/6 mice. Using image guidance, improved accuracy in treatment was observed. Mice treated with US I-PTT displayed significant improvements in tumor shrinkage and tumor-free long-term survival.[67,68]

Ye *et al.* developed NPs combining the phase-transition material perfluorohexane (PFH) with dextran sulfate (DS). The results showed that the carrier can undergo phase transition under irradiation with low-intensity focused ultrasound (LIFU), which can induce the apoptosis of macrophage cells under ultrasound imaging to achieve specific diagnosis and targeted treatment of vulnerable plaque for atherosclerosis.[69,70]

Microbubbles and nanoparticles as ultrasound contrast agents. Research applications of nanodrug delivery have been transformed through the implementation of contrast agents in US imaging. Microbubbles represent the main composition of traditional US contrast agents, while their structure includes gas-filled spheres surrounded by stabilizing shells. The echogenic properties of blood or tissues exhibit improved visualization because these microbubbles generate robust acoustic reflections. Microbubbles show exceptional value in vascular studies along with flow examinations because they stay inside blood vessels but enhance images where blood flow increases or vascular permeability occurs, such as tumor regions.[71]

NPs represent a flexible solution that has superseded traditional microbubbles as the new choice for US techniques. The development of NPs as ultrasound contrast agents offers multiple advantages over traditional microbubbles, because they overcome their limitation of poor extravasation capability. Engineered NPs equipped with tailored dimensions, electric charges, and protective coatings now enable the process of tissue penetration through bio-barriers, which include the tumor microenvironment and blood–brain barrier for precision imaging of these regions.[72]

Scientists attach targeting ligands made of antibodies or peptides to NPs, which enhances their selective build-up in designated tissues. NPs are equipped with tumor-specific ligands to create binding agents that enhance sensitive tumor cell detection. The therapeutic function of certain NP-based contrast agents allows them to act as theranostic systems with imaging drug delivery capabilities or hyperthermia activation features.[73]

Researchers have established novel methods for improving nanodrug delivery through the combination of NPs with US-mediated therapies. Therapeutic agents may penetrate target tissues more effectively through the use of focused US, as this technology produces cavitation in microbubbles and NPs, which creates mechanical forces for barrier disruption. The

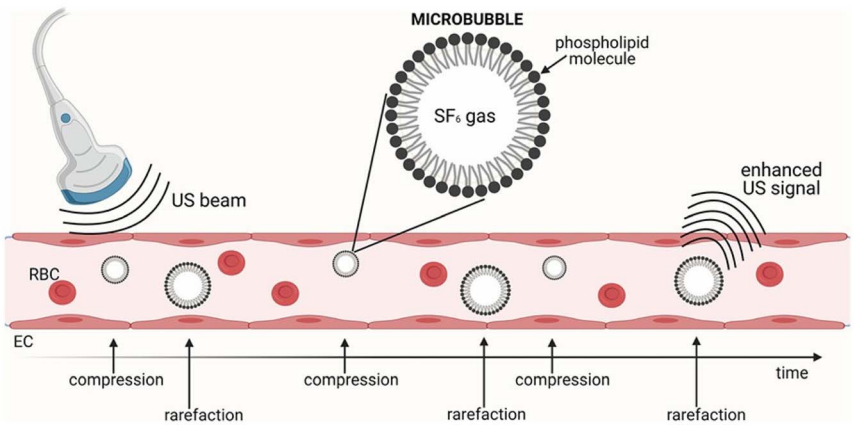

Fig. 5 Schematic representation of the mechanism of action of contrast-enhanced ultrasound using an intravenously administered contrast agent.[67] Reproduced from ref. 67.

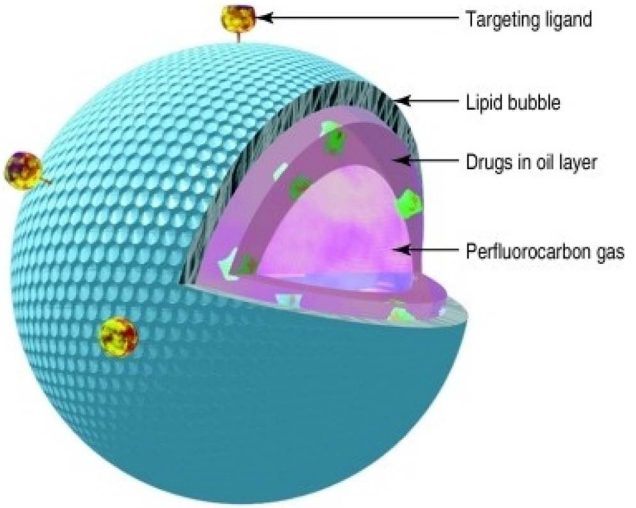

Fig. 6 Diagram of a microbubble constructed for drug delivery.[74] Reproduced from ref. 74. With permission from the BMJ.

technique shows high success in enhancing drug transport to solid tumors, which present dense extracellular matrices and limited vascularization. Although US contrast agents that use microbubbles with NPs show great potential, they continue to experience stability problems during traversal of the bloodstream and to produce unwanted extracorporeal responses. Ongoing research in material science and surface engineering will solve the issues with current agents through the production of novel, robust, and biocompatible agents.[74,75] The use of microbubbles and NPs as US contrast agents represents an essential step forward that enables better diagnostic and therapeutic possibilities through imaging-guided nanodrug delivery (Fig. 6).[74]

Hybrid and multimodal imaging

MRI-PET. A significant breakthrough in hybrid imaging was achieved through the merger of MRI and PET.[75] This breakthrough combines the benefits of MRI in terms of spatial resolution and soft tissue contrast with molecular sensitivity and the specificity of PET. Combination MRI-PET systems allow scientists to collect functional and anatomical information at the same time, which generates complete knowledge about NPs during nanodrug delivery. The combination of MRI with PET provides essential imaging capabilities that matter greatly for developing precise molecular profiles of tumors.[76]

MRI-PET technology offers superior capabilities to track NP transport through the body and measure both how NPs spread throughout the body and their capacity to fight diseases. The use of ^{18}F radionuclides on NPs enables *in vivo* PET tracking, while MRI generates detailed maps of tumors together with their tissue environments. NP targeting efficiency and drug release kinetics become assessable in real-time through the combination of these modalities. The ability to monitor these processes provides essential information for improving therapeutic results when designing NPs. MRI-PET imaging expands capabilities to monitor tumor microenvironment characteristics, including hypoxia and angiogenesis, which directly influence tumor advancement and resistance development.[77]

In another study, PET imaging enabled hypoxia-related marker assessment through ^{18}F-fluoromisonidazole (^{18}F-FMISO) tracer application, while MRI simultaneously provided information about vascular perfusion and tissue oxygen status. The purpose of this work was to examine the outcomes of spectrum analysis (SA) and compartmental modeling (CM) produced using dynamic ^{18}F-FMISO tumor images. Additionally, the dynamic models and the standard tissue-to-blood ratio (TBR) images were generated and contrasted. The ^{18}F-FMISO tracer was used for PET/CT imaging in nine glioblastoma patients. The tumor images displayed distinct patterns of hypoxia and necrosis as a function of the PET scanning periods, but the dynamic PET-imaging-based CM and SA techniques equally located tumor hypoxia. All patients' Ki scans showed an average correlation of 0.63 ± 0.19 (0.24–0.86) between CM and SA. In contrast to SA, which generated accumulation component pictures that were clearer than those of CM, CM produced Ki images that were less noisy. There was a correlation between TBR pictures and CM-Ki and SA-Ki images ($r = 0.72 \pm 0.20$ and 0.56 ± 0.26, respectively). The image revealed a strong uptake in the necrotic region in the lone patient with a continually growing tumor time–activity curve, which was not seen in the TBR or Ki images.[78]

Tu *et al.* showed that this method was feasible by using MMP2cNPs as PET-MRI contrast agents to identify MMP-2 in atherosclerotic plaques. In CL57/BL6 mice, carotid ligation combined with a high-fat diet and streptozotocin-induced diabetes resulted in macrophage-rich vascular lesions. Magnetic NPs were derivatized with NOTA for labeling with the nuclear tracer ^{64}Cu and the with MMP-2-cleavable peptide modified with polyethylene glycol 2000 (PEG 2000) to make IONP specific for the extracellular MMP-2. This results in a multi-modality formulation (^{64}Cu-NOTA-IONP@MMP2c-PEG2K, MMP2cNPs) for PET/MR imaging. According to biodistribution data and PET imaging in small animals, the MMP2cNPs demonstrated exceptional plaque uptake. Additionally, the MMP2cNPs were quickly removed from the contralateral normal carotid artery, producing outstanding contrast between the plaque and the normal carotid artery. Additionally, as compared to the agent with the non-cleavable reference molecule, MMP2ncNPs, *in vivo* MRI revealed the preferential build-up of MMP2cNPs in atherosclerotic lesions.[79]

Cowan *et al.* created a method for cardioprotection using labeled mitochondria. To enable PET and MRI detection, mitochondria were labeled with fluorine-18-rhodamine 6G (^{18}F-R6G) and IONP. In the ischemic left ventricle, the ^{18}F-R6G-labeled mitochondria produced a distinct PET signal and a T2-weighted MRI signal. The MRI and PET signals were absent from the typical right ventricle. This method may lessen cell loss, improve post-ischemic contractile performance, and shrink infarct size to preserve the heart. Infarct size was much smaller in mitochondria-transplanted hearts than in normal hearts.[80]

MRI-PET imaging involves several limitations because it requires specialized facilities, has a high cost premium, and involves the operation of complex systems. The development of tailored multifunctional NPs, along with technological improvements in hybrid scanners, will serve as driving factors for MRI-PET adoption in nanomedicine. Research-based nanodrug delivery benefits tremendously from the unified presentation of anatomical, functional, and molecular data by MRI-PET systems.

CT-MRI. Hybrid CT-MRI systems unite two complementary modal imaging techniques to deliver a strong platform for combined imaging procedures. CT delivers detailed anatomical scans of hard tissues, especially bone, while MRI shows outstanding capabilities to display soft tissue structures. The joint application of CT with MRI produces thorough NP assessment throughout both soft and hard bodily tissues, which proves essential for preclinical and clinical nanodrug delivery research.[81]

CT-MRI systems deliver exceptional performance in monitoring the movements of bone-specific drug-delivery NPs as well as those used in complex anatomical territories. The use of CT and MRI scanners together enable studies to monitor calcium-phosphate-based NP distribution throughout bone tissue in addition to tracking their potential effects on adjacent soft tissue structures. The dual abilities of these systems create a complete observation method to study NP-biological system interactions, thus enabling optimal drug delivery optimization. Medical researchers deployed CT-MRI imaging for detecting the physiological pathways of nanotechnology-based drugs through tumors and their therapeutic properties in oncology treatments. The combination of CT and MRI contrast agents in single hybrid NPs improves imaging sensitivity and specificity, and results in precise tumor localization and drug release monitoring. CT-MRI systems combine the capability to assess cancer blood vessel health while monitoring alterations in soft tissue and hard tissue characteristics due to treatments to evaluate therapy results.[82]

Lee *et al.* administered ^{99m}Tc-labeled dextran-coated SPIONPs (^{99m}Tc-SPIO) intravenously (i.v.) or intra-arterially (i.a.) with/without Lipiodol to a rabbit liver tumor and compared tumor localization using gamma scintigraphy, SPECT, and MRI. Every animal underwent two MRI scans: a first MRI one day before the distribution of ^{99m}Tc-SPIO, and a second MRI following the capture of nuclear pictures. The animals were placed into a SPECT/CT scanner and given a dynamic scan with a gamma scintigraphy picture utilizing one-minute time frames for 20 min after the administration of ^{99m}Tc-SPIO. Images from static scintigraphy were taken 60 and 180 min after delivery. The step-and-shoot scan mode was used to obtain the gamma scintigraphy images using a low-energy, high-resolution collimator. For each group, SPECT/CT scanning was carried out for 90 min following the administration of ^{99m}Tc-SPIO. CT and SPECT images were obtained for 10 and 20 min, respectively. The step-and-shoot scan mode of a low-energy, high-resolution collimator was used to capture SPECT images. SPECT/CT and gamma scintigraphy images were rebuilt using a Butterworth filter and ordered subset expectation maximization. The program automatically fused the CT and SPECT images. This combined imaging technique demonstrated the higher tumor uptake ratio of ^{99m}Tc-SPIO with Lipiodol i.a. as compared to the normal liver parenchyma and a consistent signal decrease pattern in the liver MRIs. Three hours following i.a. administration of ^{99m}Tc-SPIO with or without lipiodol, the normal liver showed diffuse uptake on scintigraphy and SPECT images and minor signal declines in the liver MRIs. This may occur if SPIO is deposited and enters systemic circulation. Chemoembolic material administration (^{99m}Tc-SPIO with Lipiodol) was tracked using nuclear medicine imaging modalities, CT, MRI, or multimodal detection, as well as fluoroscopy guidance. Image-based research confirmed that intra-arterial distribution of SPIO with Lipiodol may be an effective drug delivery strategy for hepatic malignancies.[83]

Hybrid CT-MRI imaging benefits patients through multiple advantages, but continues to face equipment costs and complicated image registration techniques as main obstacles. Scientists are devoting research efforts toward developing NP-based contrast elements that function well with both CT and MRI systems. CT-MRI maintains its value as an essential tool for nanodrug delivery research despite the current operational challenges.

Optical imaging with nuclear modalities

Another innovation in hybrid imaging was achieved through the combination of optical imaging with the PET and SPECT nuclear modalities, which use optical methods for high spatial resolution with nuclear techniques for molecular sensitivity. This multi-scale imaging method lets researchers observe the same NPs in both cellular environments and whole-body frameworks at the same time. The molecular activity of the NPs becomes visible in real-time through optical approaches, including fluorescence and bioluminescence imaging. The combination of PET or SPECT with these methods enables scientists to establish connections between NP interactions at the cellular level and their distribution throughout the body.[84] Scientists use NPs bearing combined fluorescent dyes and radiotracers to track the particles through both imaging modalities, thus achieving a complete assessment of therapeutic targeting alongside efficiency monitoring. The study of tumor-targeting NPs uses optical-nuclear hybrid imaging techniques as an important medical application. NPs enabled dual imaging of tumor accumulation and molecular interactions with their fluorescent labels and the radiotracer functions of ^{64}Cu or ^{124}I. The technique assisted researchers in tracking gene-editing instruments, including CRISPR-Cas9 systems, thus revealing their position and operational behavior.[85]

Shi *et al.* developed a yolk/shell-structured silica nanosystem for tumor vascular targeting and dual-modality PET/optical imaging. Following radiolabeling, 4T1 tumor-bearing mice received i.v. injections of the nanocomposite for PET imaging and *in vivo* vascular targeting. It showed higher targeting specificity, better imaging capabilities, and more accurate diagnostic outcomes. Because radioisotopes and chelators detach from NPs as they circulate in the bloodstream,

accumulate in the liver and other organs, and interact with proteins and other biological macromolecules, PET imaging, despite its high sensitivity and quantitative capabilities, can only depict the biodistribution of radioisotopes rather than the NPs. To verify the precision of PET imaging and show the true biodistribution of NPs, a different imaging modality is thus advised. Fluorescence imaging was used to determine the biodistribution of the nanocomposites using quantum dot (QD) NPs inside each silica shell. To further confirm their biodistribution, the anticancer drug DOX that was injected into the hollow of the nanocomposites was also imaged. The effective targeting of the nanosystems was validated by optical imaging of QD and DOX, which showed a good correlation with PET imaging. These nanosystems can be used as a multifunctional nanoplatform for drug delivery and dual-modality cancer diagnostics. By integrating vascular targeting, pH-sensitive drug administration, and dual-modality imaging into a single platform, the developed yolk/shell-structured silica nanosystems could be used for future image-guided tumor-targeted drug delivery as cancer theranostics.[86]

A new perfluoropolyether (PFPE) nanoemulsion containing a water-insoluble lipophilic drug was developed by O'Hanlon *et al.* The formulation makes it possible to use NIR optical imaging and ^{19}F MRI as non-invasive imaging modalities to track the biodistribution of nanoemulsions. Hydrocarbon oil, surfactants, NIR dye, PFPE-tyramide, and an ^{19}F MRI tracer made up the nanoemulsion. Celecoxib, a model nonsteroidal anti-inflammatory medication (NSAID), was added to the formulation at a concentration of 0.2 mg mL^{-1}. The reported nanoemulsion is an appealing prospective theranostic agent for cancer imaging and therapy due to its tiny particle size, visibility under ^{19}F MRI and NIR fluorescence spectroscopy, and drug-carrier capabilities. The research showed that the theranostic nanoemulsion, which carries a water-insoluble medication with an intracellular target, the COX-2 enzyme, can be administered to cells and make them visible by both ^{19}F MRI and NIR.[87]

Hybrid nanoconstructs that can be injected intravenously have been created to reduce systemic and local immune cell inflammation. For combined nuclear/optical imaging, lipid and polymer chains are nanoprecipitated to create 100 nm spherical polymeric nanoconstructs (SPNs), loaded with methotrexate (MTX), and then tagged with ^{64}Cu and fluorescent probes. A particular build-up of SPNs within lipid-rich plaques along the arterial tree was observed *via* nuclear and optical imaging in ApoE−/− mice that were given a high-fat diet for up to 17 weeks.[88]

The benefits of optical–nuclear imaging coexist with two main drawbacks, namely, the restricted penetration of optical signals into tissue and the potential signal cross-interference between the different modalities. Scientists have addressed the limitations of these imaging systems by creating near-infrared fluorescent probes and optimizing radiotracer combinations to achieve better outcomes. Future technological developments in hybrid imaging probe structures coupled with improved data fusion methods will extend the research capabilities of optical–nuclear imaging for nanodrug delivery applications. This methodology unites optical and nuclear modalities through a strong framework that enhances both NP research capabilities and clinical therapy results.

Effect of nanoparticles on imaging signal generation and transmission

NPs are revolutionizing medical imaging by improving the clarity and precision of signals. Their distinct physical and chemical characteristics allow them to scatter or absorb light, sound, or radiation in ways that improve the creation and transmission of images. Unlike conventional contrast agents, these microscopic particles may be engineered to go straight to the location of the disease, aiding in the more efficient highlighting of trouble spots. Imaging becomes more precise, comprehensive, and helpful for early diagnosis and treatment planning as a consequence.[89]

Smart contrast agents for MRI can be developed using uSPIOs. Commercially available oleic-acid-capped uSPIOs are hydrophobic, which prevents them from being used *in vivo*. It is possible to make uSPIOs water-soluble, biocompatible, and extremely stable in physiological settings by using a hydrophilic ligand that has a strong affinity for their surfaces. The optimal pharmacokinetics and tumor delivery patterns, and, most importantly, improved T1 MR contrasts are guaranteed by a reduced overall hydrodynamic diameter. With a typical core size of 20–50 nm, nanoscale SPIO has long been used as a T2 contrast agent for MRI. Interestingly, various factors cause the SPIO core to display greater T1 enhancement when its size is reduced to less than ∼5 nm: (i) Multiple Fe^{2+}/Fe^{3+} ions are exposed to water protons dispersed *via* the hydrophilic layer by a high surface-to-volume ratio, which reduces their longitudinal relaxation time by giving them empty orbits; (ii) ultrasmall NPs with a fast correlation time further boost T1 relaxation processes. Several investigations have demonstrated encouraging T1 enhancement patterns using sub-5-nm uSPIOs.[90]

The remarkable susceptibility and relaxivity of SPIONs in ultra-low field (ULF) regimes make them a suitable contrast agent for ULF MRI. In ULF environments, the magnetic field dependency of the relaxivity of SPIONs is very beneficial. The transverse-to-longitudinal SPION relaxivity ratio approaches unity at ultra-low magnetic fields, and the relaxivity of SPIONs is noticeably higher than at higher magnetic fields (>1.0 T).[91] Because of these two characteristics, SPIONs are a viable option for producing positive contrast at ULF. Furthermore, at ULF, SPIONs retain their high magnetic susceptibility, while the magnetic susceptibility of the human body decreases to almost zero. This produces basically background-free susceptibility contrast, which is a useful characteristic for susceptibility-related MRI. Sample characterization and phantom imaging have shown that SPIONs have increased relaxivity at ULF.[92]

Under structured illumination, the NPs exhibit stability, uniformity, and brightness, supporting a lateral resolution of 186 nm, which is less than 1/4th of the excitation wavelength. By resolving the particles within the optical limit, the enhanced resolution allows for better multiplexing capacity in space and high throughput. Super-resolution imaging using super-

resolution microscopy (SRM) is aided by these time-domain super-resolution multiplexing NPs.[93]

Traditional contrast agents for CT are mostly tiny compounds with several drawbacks including poor targeting in tumors and human circulation and fast metabolism that restrict their therapeutic effectiveness. Because of the special qualities, such as surface modifiability and enhanced permeation and retention (EPR) in solid tumors, nanoformulations have attracted a great deal of interest in fundamental research into disease diagnostics and therapy. By combining the potential benefits of nanomaterials, research into the creation of more focused nano-enhanced contrast agents seeks to address the drawbacks of conventional small-molecule contrast agents. Enhancing the diagnostic capacity and quality of medical imaging has emerged as a key research topic in the development of contrast agents with improved medical imaging capabilities.[94] High structural stability, good biocompatibility, high water solubility, powerful targeting, regulated retention, and slow metabolism are the five qualities of ideal CT contrast agents. Effective drug manufacturing requires high water solubility, biocompatibility, and structural stability. The slow metabolism, strong targeting, and regulated retention of a contrast agent enable it to stay at the target location for the expected amount of time, greatly increasing diagnostic sensitivity and effectiveness. Research into nano-CT contrast agents is now primarily focused on processing high-atomic-number materials to the nanoscale, analyzing and altering these materials for various anatomical locations and illnesses, and creating nano-targeted reagents to accomplish these five features.[95] Among the various developments in nanomaterials, metal-based inorganic NPs with substantial X-ray attenuation coefficients and high atomic numbers have the potential to be used as CT contrast agents in specialized bioimaging. As of right now, a variety of contrast agents for CT imaging have been documented, including nanomaterials based on gold (Au), bismuth (Bi), lanthanides (Ln), and transition metals (TM), among others.[96]

Currently, contrast-enhanced ultrasonography (US) is employed around the world for clinical purposes in radiology and cardiology, and it continues to develop thanks to creative technical breakthroughs. Recent research has demonstrated the imaging potential of nanobubbles by fusing their special qualities with the concepts of ultrasonic imaging. With recent research showing novel imaging applications, contrast-enhanced ultrasonic imaging utilizing these agents continues to gain popularity. The primary benefit of employing NBs for US imaging is that it represents an innovative way to combine the remarkable safety profile and affordability of US with the extravascular access of nanoscale agents. Because NBs may pass through microcapillaries at relatively high concentrations and pass through the vascular endothelium in the presence of leaky vasculature, they can be used in novel imaging applications.[97]

In photoacoustic imaging (PAI), optically absorbent materials are excited by a pulsed laser light source, resulting in temporary, localized heating. Thermal expansion brought on by the temperature rise produces pressure waves, which may be examined to provide compositional and spatial details about the area being photographed. Plasmonic NPs are potential contrast agents for PAI because of their adjustable optical extinction cross-sections, which are several orders of magnitude greater than those of endogenous materials. A nanosecond laser pulse is "long" in relation to the time of heat conduction within the NPs because of the small size and high thermal conductivity of metal NPs, which cause the heat generated within them to be distributed evenly throughout their volume in picoseconds. Additionally, the PA signal is mostly produced in the fluid that surrounds it rather than inside the NP itself. Furthermore, compared to that of dispersed silica-coated AuNPs, the PA signal from aggregated silica-coated AuNPs is significantly increased. These findings have significant ramifications for the use of plasmonic metal NPs in quantitative molecular imaging, as cellular uptake and endocytosis lead the particles to aggregate.[98]

AuNPs offer great PA contrast and a large absorption cross-section based on surface plasmon resonance. Because AuNPs may be functionalized to target important molecular locations of interest and distribute themselves at specific cell sites, they also allow for targeted specificity. The majority of the PA signal creation happens in the surrounding biological fluid, into which the absorbed energy quickly diffuses when an AuNP generates a PA signal *via* light absorption. Extreme heating of the nano-scale fluid volumes surrounding the AuNPs causes changes in the thermal expansion coefficient of the surrounding environment, which is why some AuNP colloids, such as nanospheres larger than 100 nm in diameter in water, show nonlinear PA signal strength with respect to excitation fluence. The PA signal is proportional to the thermal expansion coefficient, which results in the nonlinear PA signal production phenomena.[99]

Emerging techniques and future trends

AI has proven to be very accurate and efficient in supporting biomedical imaging in medical decision-making for both cancer and non-cancer treatments. With their high contrast, low cost, and non-invasive nature, optical imaging techniques in particular can be used to diagnose and view the structural and functional information of diseased tissues. The early detection of cancer and non-cancer disorders is not supported by the traditional diagnostic methods used in the modern medical field. Thus, there is a pressing need to create early diagnosis tools through the synergistic use of AI with cutting-edge biomedical imaging technologies like SRM and PAI. However, by utilizing computer vision, deep learning (DL), and natural language processing (NLP), AI may direct optical imaging techniques to increase the precision of disease identification, automated analysis and prediction of its histopathological section, monitoring during therapy, and prognosis.[100]

Because it is highly sensitive to metabolic changes, photoacoustic spectroscopy (PAS) can be used to identify a variety of disorders *in vivo*. Clinical applications that include PAS can greatly improve diagnostic skills and offer vital molecular insights into health and illness. Additionally, by calculating tissue metabolism and chromophore composition, optical

inversion of PAI may be carried out. The optical characteristics of the sample (tissue), including the absorption coefficient, can be computed using optical inversion. The concentration of various compounds in the tissue is then calculated using these characteristics. This method is known as quantitative PAI, and while it is more difficult than acoustic inversion, it may yield more precise tissue information. When combined with AI, especially DL, this method is a promising field of study. With a greater understanding of the alterations in biochemical processes at the outset of the disease, this PAS potential enables molecular-specific imaging and functional investigation of disease states.[101]

In terms of spatial resolution, SRM surpasses the diffraction limit of traditional light microscopy. It is becoming more and more significant in the life sciences, as it offers new spatial or spatiotemporal information on biological processes at molecular specificity and nanoscale precision. However, because of its technological constraints, trade-offs must be made in order to balance the light exposure of the samples, temporal resolution, and spatial resolution. DL has recently demonstrated ground-breaking performance in a variety of computer vision and image processing tasks. Additionally, it has demonstrated great potential in expanding the SRM performance envelope.[102]

To enhance the delivery of nanodrugs *in vivo* and observe these drug carriers both inside tissues and at incredibly tiny cellular levels, researchers are increasingly concentrating on combining the state-of-the-art imaging techniques PAI and SRM with AI. A larger change in medical science, in which the objective is to create more precise, dependable, and focused methods for monitoring and directing treatments, is reflected in the increasing interest in combining various imaging systems with AI. Plans for safer and more effective medicine delivery are being shaped by the continuous developments in this field. The efficiency and accuracy of nanodrug delivery in cancer and non-cancer disease tissues are improved by PAI, SRM, and AI imaging techniques, which we have briefly covered in the section that follows.

Photoacoustic imaging

PAI represents an advanced imaging technology that unites optical and US methods to generate high-definition subsurface scanning. PAI generates US waves through its mechanism, which stimulates tissues with pulsed laser light and triggers transient thermoelastic expansion. The detected signals help engineers to produce detailed images of biological frameworks.[103]

PAI has proven to be essential for tracking NPs as they move throughout the human body during nanodrug delivery procedures. The detection of drug carriers benefits from the incorporation of NPs that utilize strong optical absorption from materials like gold nanorods or carbon-based nanomaterials. The PAI technique enables unique applications in cancer research, as it helps researchers to observe how NPs are distributed inside tumors, measure blood vessel growth, and monitor treatment effectiveness instantly. PAI allows researchers to combine imaging functions with MRI or US modalities so that both structural and functional information becomes available.[104]

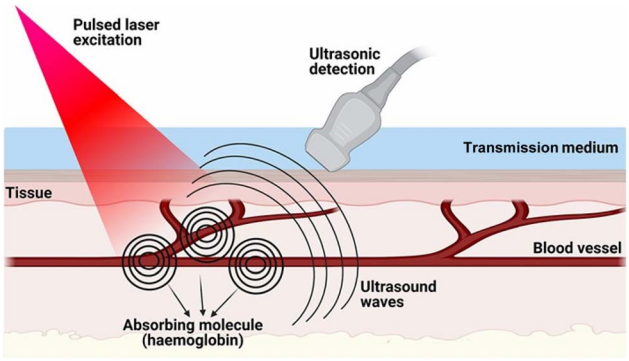

Fig. 7 Schematic representation of the mechanism of action of photoacoustic imaging.[67] Reproduced from ref. 67.

The successful application of PAI faces limitations, because researchers need to enhance the properties of contrast agents as well as improve their tissue penetration depth. Research teams are currently working on creating optimized NP design techniques that focus on improving imaging systems to increase the potential clinical ramifications of PAI.[104,105] Theranostic applications of PAI show promise to become an important diagnostic device bridging optical and US imaging technology (Fig. 7).[67]

Chen *et al.* used siRNAsT/I and PBNPs to suppress the proinflammatory cytokines TNF-α/IL-6 and reduce ROS levels in RAM. The nanocomposite was monitored *via* NIR PAI. Furthermore, multispectral PAI without the necessity for labeling enabled the real-time assessment of the nanocomposite as a potential rheumatoid arthritis therapy.[105,106] Kubelick *et al.* combined the US and PAI techniques to track T cells after adoptive transfer for cancer treatment. The *in vivo* US/PAI method detected NP-labeled T cell accumulation at the tumor, showed changes in tumor volume, and relayed associated changes in blood biomarkers. The results emphasize the potential of the method and encourage future research to broaden the platform for advanced theranostic immunoimaging.[107]

Gold–selenium core–shell nanostructures (AS-I/S NCs) with good NIR-II PAI were designed for myocardial ischemia-reperfusion injury (MI/RI) treatment. The *in vivo* administration of AS-I/S NCs dramatically improved myocardial function and angiogenesis and inhibited myocardial fibrosis by inhibiting myocardial apoptosis and oxidative damage in the MI/RI of rats as demonstrated by NIR PAI.[108] A π-conjugated polymer (PMeTPP-MBT) based on 3,6-bis(4-methylthiophen-2-yl)-2,5-bis(2-octyldodecyl)pyrrolo[3,4-*c*]pyrrole-1,4(2*H*,5*H*)-dione was designed as a novel PA contrast agent. On this basis, an intelligent responsive theranostic nanoplatform (PA/ASePSD) combining astaxanthin and SS-31 peptide and loaded with PMeTPP-MBT was developed. Both *in vitro* and *in vivo* evaluations confirmed the impressive anti-atherosclerotic capability and the accurate photoacoustic diagnosis of the PA/ASePSD

NPs, thus making them a promising candidate for early-stage atherosclerosis theranostics.[109]

Super-resolution microscopy

Super-resolution microscopy (SRM) represents a major improvement in optical imaging as it overcomes the diffraction limit barrier of standard light microscopy. Research techniques including stimulated emission depletion (STED), structured illumination microscopy (SIM), and stochastic optical reconstruction microscopy (STORM) allow scientists to study the visual characteristics of NPs and their cell interactions at microscopic resolution.[110]

SRM is a promising research technique to observe the intracellular pathways of NPs during studies of nanodrug delivery. The sub-diffraction-limit resolution of SRM reveals the path of NPs as they travel through cellular structures, including endosomes, lysosomes, and the nucleus. The optimization of NP design requires this capability to ensure effective drug release at target sites.[111]

SRM serves as a useful tool for scientists investigating how NP uptake mechanisms intersect with biomolecule interactions. Scientists have utilized STORM imaging approaches to study how NPs modified with ligands interact with cellular receptors until receptor-based signals activate their response pathways. The discovered insights are used to design rational drug delivery systems with better therapeutic effects. SRM has revolutionized nanoscale imaging, but it still faces several obstacles including photobleaching, low data processing speed and technologically complex analysis. Biomedical research will benefit from the ongoing development of projects to improve fluorescent probes and image acquisition speed while establishing methodologies combining SRM and other imaging platforms. Super-resolution techniques show advancing potential for nanodrug delivery and precision medicine as they continue to develop.[112,113]

Andrian *et al.* suggested a correlative light and electron microscopy (CLEM) technique that combines direct stochastic optical reconstruction microscopy (dSTORM) with transmission electron microscopy (TEM). The authors combined these techniques to precisely locate NPs in the target cell. Individual fluorescently labeled poly(lactide-*co*-glycolide)-poly(ethylene glycol) (PLGA-PEG) NPs were observed immediately with dSTORM and allocated to cellular compartments using TEM. Initially, the NPs were monitored *via* the endo-lysosomal route at various time intervals, and the influence of chloroquine on their intracellular distribution (endosomal escape) was then demonstrated. These investigations are of considerable significance to gather key information on NP trafficking, and critical for the creation of increasingly complicated NPs for cytoplasmic/nucleic medication delivery.[112]

Targeted NP treatment *in vivo* was shown using Sn-2 lipase labile phospholipid prodrugs in conjunction with the contact-facilitated drug delivery method. The study clarified the intracellular trafficking and metabolic features of PC prodrugs for the first time using single-molecule super-resolution imaging methods. Through both ATP-dependent and ATP-independent methods, PC prodrugs are translocated to the inner membrane leaflet after being widely integrated into the outer cell membrane leaflet over the cell body and filopodia. Instead of being enclosed in endosomal vesicles, the PC prodrugs that were introduced into the cells filled the vesicle membranes, which then moved to the perinuclear Golgi/ER area and dispersed across the intracellular membranes of the cytosol. In contrast to the general cytosol, the DOX-prodrug was tracked to the Golgi/ER area, where the greatest level of released drug was recorded. This work offered the first evidence-based understanding of the fate of the intracellular Sn-2 PC prodrug, even though the specific fluorescence lifetimes examined in this investigation had little correlation with values for *in vivo* imaging.[113]

Chen *et al.* showed the use of a novel SIM technique to investigate the biological effects of medications; specifically, they discovered therapeutic interactions with mitophagy. Additionally, this work more accurately demonstrated that mitochondrion–lysosome interactions occur in live cells.[114]

Artificial intelligence

Faster, more accurate, and comprehensive interpretation of complex imaging datasets is now being achieved using AI, which represents a dynamically changing paradigm in the field of imaging analysis. Machine learning (ML) algorithms, especially deep learning, are particularly powerful tools for pattern recognition, image segmentation, and feature quantification, especially when human interpretation would otherwise be difficult or time-consuming. AI is used to analyze multi-modal imaging data from modalities such as CT, MRI, PET, and optical imaging, offering insights into NP behavior and therapeutic outcomes in nanodrug delivery research.[115]

There are many potential applications of AI in the area of nanodrug delivery. One major example is in the automated segmentation and tracking of NPs *in vivo*. Trained algorithms utilize annotated datasets to dissect the biodistribution, accumulation, and clearance of NPs based on their respective models. This works especially well for studies that span several years and generate significantly more imaging data than conventional analysis can typically handle. AI permits multi-modal imaging data integration to reveal anatomical, functional, and molecular correlative behaviors of NPs. AI algorithms, for example, are capable of integrating PET and MRI data to determine the delivery efficiency and therapeutic effect of radiolabeled NPs, which speeds up the analysis procedures and increases the accuracy.[116]

Chou *et al.* developed an AI-assisted physiologically based pharmacokinetic (PBPK) model by combining an AI-based quantitative structure–activity relationship (QSAR) model with a PBPK model to predict the biodistribution of different NPs and tumor-targeted delivery efficiency (DE). ML and deep neural networks were used to develop an AI-based QSAR model, which was trained on datasets from a public Nano-Tumor Database to forecast important input parameters for the PBPK model. The predictions of the AI-PBPK model agreed well with pharmacokinetic features obtained experimentally from intravenous

administration of NPs in tumors. The AI-based PBPK model offers a useful screening tool to quickly predict the distribution efficiency of NPs based on their physicochemical characteristics without relying on an animal training dataset.[117]

Using light sheet fluorescence microscopy and a deep learning-based image analysis technique, Yang *et al.* presented LungVis 1.0, an AI-powered imaging ecosystem that maps NP deposition and dosage quantitatively and holistically across the bronchial and alveolar (acinar) regions in murine lungs for widely used bulk-liquid and aerosol-based delivery methods. The researchers demonstrated that although aerosols accomplish uniform deposition to distant alveoli, bulk-liquid injection results in an uneven NP distribution with high bronchial dosages. Additionally, the authors contradict the conventional understanding that lung tissue-resident macrophages (TRMs) are static by demonstrating that TRMs are dynamic, continually monitoring and redistributing NPs inside alveoli. An improved framework for examining pulmonary delivery dynamics and learning more about TRM-mediated lung immunity is provided by LungVis 1.0.[118]

To evaluate the utility of drug-controlled release in liver cancer patients, the supplemental function of a convolutional neural network (CNN)-based MRI image segmentation algorithm in MRI image-guided targeted drug treatment with DOX-loaded NPs was examined. Eighty people with liver cancer were selected as research participants for this study. To evaluate the imaging analysis impact of this algorithm on the targeted treatment of liver cancer with DOX-NPs, it was anticipated that the CNN-based MRI image segmentation algorithm could be used to direct the analysis of MRI images of the targeted controlled release of DOX from NPs. The findings of the study demonstrated that the improved 3D CNN-based MRI image segmentation outperformed the conventional CNN-based MRI image segmentation, with notable gains in metrics including sensitivity, specificity, accuracy, and precision. Further, all of the differences were statistically significant.[119]

In electron microscopy analysis, AuNPs may also be employed as immunolabels to help to identify proteins and examine their density and location within cells. Recently, Jerez and colleagues built a free DL-based program called Gold Digger that allows for speeding up and reducing the annotation mistakes caused by human picture analysis for a more accurate result. Additionally, AuNPs are frequently used to track the effectiveness of treatment and test for illnesses in asymptomatic people.[120]

Cell internalization of NPs as a diagnostic method for breast cancer detection was assessed in another investigation. The majority of cancer-related fatalities are caused by metastasis. The ability to compare the absorption of NPs into micrometastases to that of the main tumors was made possible by an ML-based image analysis linked to tissue clearance and 3D imaging. Furthermore, ML made it possible to accurately anticipate how the pathophysiology of micrometastases would affect the transport of NPs. This aids in determining how patients react to particular therapies.[121]

Harmony of multimodal imaging systems for enhancing the efficiency and precision of nanomedicine drug delivery

Combining the advantages of many imaging modalities while overcoming their drawbacks is made possible by multimodality imaging, which uses two or more imaging methods. Specifically, it has been demonstrated that combining structural and functional imaging with integrated SPECT/CT and PET/CT is very beneficial and efficient.[122] The desired goal of a multimodal imaging technique is to accurately visualize the specific location, metabolic activity, and molecular pathogenic causes of the target organ or tissue. As a result, it promises significant advantages for enhancing sickness detection and treatment evaluation.[123]

One unmet need in oncology is the development of multimodal systems for neoplastic disease detection and treatment. In addition to enabling acoustic imaging, the combination of imaging and treatment capabilities, such as High-Intensity Focused Ultrasound (HIFU), has been widely used to treat some primary solid tumors and even metastatic cancer. This has improved the therapeutic effect and allowed diagnosis and treatment to be integrated. Hybrid NPs were prepared by Novoselova *et al.* using biocompatible polymers, magnetic NPs (MNPs), photoacoustic and fluorescent components, and DOX. The resultant device offers HIFU-mediated drug release at the site of interest, strong contrast in high-resolution MRI, optoacoustic, and fluorescence imaging, and the ability for particles to transverse a magnetic field gradient. The presence of magnetite NPs for MRI, a fluorescent dye for fluorescence tomography, and photoacoustic properties allow for the visualization of these multimodal particles. Using the clinically authorized HIFU approach can enable site-specific polymer shell disintegration and release of the therapeutic drug, such as DOX, after particle accumulation in the organ of interest has been confirmed.[124]

Guo *et al.* reported PFH-PTX@PLGA/SPIO-Her as a NIR light-controllable, targeted, and biocompatible drug delivery nanoplatform for PA/US bimodal imaging-guided PTT/chemo synergistic cancer treatment of breast cancer. To direct tumor treatment, the encapsulated SPIO NPs can be used as a superior PAI tool. The SPIO might also convert NIR light into heat energy for tumor photothermal ablation when exposed to it. As a PA/US bimodal imaging agent, the photothermal-conversion nanomaterials (photothermal hyperthermia) and controllable drug delivery nanoagents (optical droplet vaporization) of the biocompatible PFH-PTX@PLGA/SPIO-Her NPs eliminated the tumor with negligible adverse effects. By utilizing the rapid evolution of nanomedicine, the theranostic approach not only combines the benefits of conventional imaging and therapeutic modalities, but also opens a new avenue for effective cancer therapy.[125]

Recently, a PET/CT probe for sentinel lymph node (SLN) metastatic imaging was created using amphiphilic polymer NPs that were radiolabeled with ^{68}Ga.[55] The higher stiffness of the used ligands was linked to the improved stability and radiolabeling yield of the NPs. In contrast to small-molecule probes based on ^{68}Ga, the significance of controlling the chelation

efficiency and stiffness of the coordination structure of ^{68}Ga-labeled NPs was examined. The PET/CT scans showed that only the strongest stiffness of coordination structure allowed for the best distinction between normal lymph nodes and tumor-metastasized SLNs. Wen *et al.* developed PET/MRI and PET/CT modes of nanoprobes based on organic NPs.[126] Dopamine–melanin NPs including biocompatible and biodegradable naturally occurring dopamine were employed as a new nanoplatform. The monoclonal antibody trastuzumab was placed on the PEGylated surface of the NPs. Human epidermal growth factor 2 (HER2) is highly favored by this antibody. PET/MRI and PET/CT imaging were used to assess the pharmacokinetics and *in vivo* behavior of the radiolabeled nanoprobe (^{124}I/^{64}Cu, Mn)-Her-PEG-dMNPs in patient-derived xenograft animal models of gastric cancer. The important conclusions of the study were reduced cardiac toxicity, improved retention duration of trastuzumab in tumors, and the potential to track the therapeutic effect in real time using dual-modality imaging.

NPs enable targeted administration of medications, genetic material, photothermal agents, and imaging agents in the context of cardiovascular disease. Imaging techniques including cardiovascular magnetic resonance (CMR), CT, PET, PA/US, and fluorescence imaging can be used to precisely direct and track the circulation of these therapeutic NPs. Non-invasive multimodal nanotheranostic systems have been increasingly in demand recently. These systems combine many imaging methods, including magnetic resonance and optical resonance, into a single NP. This platform offers hints for appropriate diagnosis and aids in the acquisition of more precise descriptions of cardiovascular disorders.[127] The use of numerous molecular imaging methods, including intravital microscopy, NP-enhanced molecular MRI, multicolor spectral CT, and fluorescence imaging, has been documented in atherosclerosis; PET has also been used to monitor and quantify blood vessel wall inflammation.[128]

For direct and non-invasive visual imaging of the ischemic myocardium in a rat model, Chen *et al.* created a targeted nanoprobe (IMTP-Fe_3O_4-PFH NPs) with improved US, PA, and MR performance. *In vivo* imaging data following NP injection into the tail veins of rat models revealed a markedly increased US/PA/MR signal, demonstrating the surprising practicality of using a nanoprobe to differentiate ischemic myocardium.[129] By integrating PAT with optical coherence tomography (OCT), Shang *et al.* were able to determine the optical absorption and scattering characteristics of vascular plaques, which were then utilized to differentiate the composition and structure of the plaques. OCT used scattering differences to acquire collagen imaging, while PAT used optical absorption differences to collect lipid information. It was shown that the combined PAT and OCT methodology might be a useful way to identify the structure and makeup of the fibrous cap and lipid core in atherosclerosis.[130] There have been reports of the use of optoacoustic (OA)/PET imaging and OA/SPECT as therapeutic agents in mouse models of stroke and Alzheimer's disease (AD).[131] The functionalized croconium dye [^{18}F]CDA-3 has been used to produce OA/PET/fluorescence triple-modality imaging of brain amyloid-β plaques, demonstrating cortical buildup of amyloid-β deposits in AD amyloidosis-affected rats.[132]

Drawbacks and challenges

Technical limitations of imaging techniques

Although nanodrug delivery has undergone transformative changes because of imaging techniques, numerous technological barriers block the complete implementation of these techniques. Challenges during imaging include poor resolution, restricted penetration depth, conflicting accuracy levels, and detector sensitivity. The tissue penetration barrier and low sensitivity levels prevent fluorescence and bioluminescence imaging from being applied to deep tissue studies. The tracking of NPs requires molecular sensitivity, which exceeds the capabilities of MRI and CT despite the excellent anatomical detail they provide. The development of specific imaging modality-optimized multifunctional contrast agents faces significant restrictions in availability.[133]

Instrument colocation is typically necessary for direct correlative multimodal bioimaging across domains, especially when *ex vivo* samples are used. However, these tools are rarely found in the same building, which complicates end user processes. To avoid these issues, it would be ideal to use a single multimodal instrument. Combining platforms is extremely difficult due to the technical requirements of molecular/structural imaging techniques and microscopy.[134] These limitations have been addressed, for instance, by combining light sheet microscopy and optical projection tomography to improve contrast for imaging model organisms and by combining quantitative fluorescence endoscopy with MRI for human and preclinical imaging to better evaluate therapeutic response.[135] Rapid label-free imaging of structural and chemical detail in tissues is also made possible by the combination of OCT, nonlinear optical imaging, and spectroscopy.[136] Because organ size, structure, and morphology vary after sample extraction, integrating *in vivo* and *ex vivo* images presents difficulties for indirect multimodal bioimaging. To lessen this, sensitive organs and tissues, such as arteries, can be meticulously preserved *ex vivo* under physiological settings.[137]

Since each imaging agent may have unique pharmacokinetic and *in vivo* biodistribution characteristics, using various imaging molecules or markers is not the best course of action. The development of trustworthy bimodal probes that are similar across imaging modalities would be aided by single markers. Recent advancements in fluorinated imaging probes for MRI have made it possible to track immune cells and perform dual structural imaging *in vivo* in a mouse model of neuroinflammation. The same probe and chemical features can then be detected at a higher resolution using Raman imaging of *ex vivo* spinal cord slices.[138] This made it possible to track inflammatory cells in real time inside certain anatomical regions, in addition to single-cell-level ambient chemical signals that aid in differentiating between healthy and sick tissue. Similarly, to facilitate the co-registration of modalities and evaluate disease heterogeneity across scales, PET/MRI

imaging of glioma mice models has been coupled with optical imaging of *ex vivo* optically cleared brain slices.[139]

Despite their enormous potential for research and diagnostics, multimodal approaches that bridge *in vivo* and *ex vivo* imaging across scales from preclinical imaging to microscopy are hindered by the challenges in hardware and software solutions to locate the same imaging region after transfer between platforms, including correlative probes and fiducial markers. A multimodal process that uses MRI, PET, CT, US, OCT, and light microscopy to observe the vasculature at various length scales and to provide molecular data on blood flow and hypoxia is an example.[140] The processes to combine these datasets and extract significant results are still difficult for novice researchers to understand, sluggish, and complicated. Research progress in PAI and hybrid imaging techniques to improve resolution limitations and molecular probe development will achieve enhanced biocompatible targeted delivery. Nanodrug delivery research will experience substantial advancements as imaging technologies continue to advance, despite the multiple research limitations.

Regulatory and ethical considerations

The medical application of imaging techniques designed for nanodrug delivery faces substantial obstacles when moving from research to clinical environments because of regulatory frameworks, as well as ethical considerations. The regulations concerning imaging agents and devices differ among geographical areas, because strict evaluation of safety and quality are required in addition to performance. Medical authorities require NP imaging probes to undergo detailed preclinical and clinical assessments to determine their safety parameters and their distribution throughout the body. The requirements slow research timelines and force manufacturers to pay higher development costs, which creates substantial barriers for both groups.[141]

The main ethical issues arise from the dangers of both the contrast agents and radiation exposure involved in medical imaging examinations. The use of gadolinium-based agents for MRI results in rare cases of nephrogenic systemic fibrosis among patients whose kidneys lack sufficient function. The use of ionizing radiation in the PET and CT modalities creates safety concerns about total radiation levels that primarily affect vulnerable groups, including pediatric patients and cancer patients who frequently need repeated diagnostic tests.[142]

The ethical aspects surrounding preclinical research emerge from animal modeling, as questions exist regarding subject welfare and study translation from animals to human participants. Any study using lab animal subjects must comply with additional ethical guidelines concerning their treatment, along with generating meaningful results to validate live model testing. Scientific research must display absolute ethical rigor in its design principles and data interpretation methods due to observed differences between preclinical results and clinical practice.[143]

The fundamental problem relates to how easily these advanced imaging technologies can reach and serve all populations. The expensive infrastructure of advanced imaging technology limits its deployment to low-resource areas, which consequently worsens healthcare disparities between regions. The ethical need for equal technology access demands coalition work between legislators, technology creators, and medical experts.[144]

Security concerns about data privacy become major obstacles, specifically in imaging analysis systems that apply AI techniques. Patient confidentiality and sensitive information safety demand tight protection measures, because large training datasets are essential for machine learning algorithms. Guidelines based on ethical principles are needed to create systems of rules for managing imaging information from acquisition through storage and distribution while protecting individual rights.[145]

Multiple stages of research involving collaborate among medical experts and legal specialists must be conducted to resolve the concerns of authorities and ethical matters. Meaningful clinical results from imaging technology breakthroughs require streamlined regulation and robust ethical standards, combined with increased investments in accessible imaging equipment. The field will reach its maximum potential together with optimal safety and equity standards through the implementation of environments that promote innovation and accountability in imaging-guided nanodrug delivery.[146,147]

Conclusion and future perspectives

Because nanodrug delivery requires innovative imaging techniques, they have taken on essential roles in helping scientists to understand NP interactions with biological systems better. This review examines multiple imaging techniques, starting from optical imaging through MRI, CT, nuclear imaging, US and new hybrid systems, in addition to their practical and restrictive elements. The molecular sensitivity of PET pairs with the high spatial resolution of MRI, while US provides real-time capabilities for vital NP studies regarding biodistribution, pharmacokinetics, and therapeutic efficacy evaluations.

Modern medical imaging combinations such as MRI-PET and CT-MRI now serve as essential tools to combine individual imaging artifacts by providing complete structural, functional, and molecular data. Innovative approaches, including PAI and SRM, along with AI-driven imaging analysis, help researchers advance nanodrug delivery standards by enabling the analysis and tracking of NPs using high-resolution methods at macroscopic and microscopic ranges.

Advancements in nanodrug delivery research face essential barriers related to technical difficulties, as well as high expenditures, regulatory requirements, and ethical obstacles. Resolving these barriers will require joint work between researchers and clinicians, as well as industry stakeholders and policymakers. The elimination of the present obstacles would enable nanodrug delivery systems with superior precision and safety to have greater clinical effects.

Nanodrug delivery imaging research will progress *via* advances in the development imaging technology development and therapeutic system unification. The future of imaging relies

heavily on multimodal techniques that unite different approaches to generate one complete picture of nanomaterial properties and therapeutic results. PAI systems connected to MRI or PET scanners provide biologists with the ability to track NP movement throughout tissues simultaneously with therapeutic effect monitoring in real-time.

Imaging analysis will adopt AI as a fundamental approach to handle complex datasets alongside multimodal imaging data integration through automated interpretation mechanisms. The utilization of AI models will aid in the development of NPs *via* their *in vivo* prediction capabilities, which speed up the creation of enhanced drug delivery systems. New developments in machine learning technology, combined with robust computational resources, will improve both the precision and productivity of research supported by imaging guidance. On a technical level, stimulus-sensitive NPs will allow the visualization of multiple therapeutic steps in real time through molecular imaging mechanisms.

Translational research for imaging-guided nanodrug delivery systems requires more attention in terms of regulatory frameworks and ethical standards. Achieving the safe deployment and widespread utilization of these technologies will require simpler regulatory frameworks as well as robust moral ones to safeguard against hindering their performance and usability. Additionally, inequalities in access to advanced imaging technologies must be addressed, as the advantages should be distributed equitably among populations and regions.

Data availability

No new data were generated during the preparation of this article.

Author contributions

Conceptualization, V. M., and Y. M.; writing—original draft preparation, V. M., N. K., A. A. A. A., and Y. M.; writing—review and editing, V. M., M. V., A. A. A. A., A. C., and Y. M.; supervision, V. M., and Y. M. All authors have read and agreed to the published version of the manuscript.

Conflicts of interest

The authors declare no conflict of interest.

References

1 R. Khanbabaie and M. Jahanshahi, *Curr. Neuropharmacol.*, 2012, **10**, 370–392.
2 S. Adepu and S. Ramakrishna, *Molecules*, 2021, **26**, 5905.
3 A. A. Yetisgin, S. Cetinel, M. Zuvin, A. Kosar and O. Kutlu, *Molecules*, 2020, **25**, 2193.
4 J. K. Patra, G. Das, L. F. Fraceto, E. V. R. Campos, M. D. P. Rodriguez-Torres, L. S. Acosta-Torres, L. A. Diaz-Torres, R. Grillo, M. K. Swamy, S. Sharm, S. Habtemariam and H. S. Shin, *J. Nanobiotechnol.*, 2018, **16**, 71.
5 V. Yagublu, A. Karimova, J. Hajibabazadeh, C. Reissfelder, M. Muradov, S. Bellucci and A. Allahverdiyev, *J. Funct. Biomater.*, 2022, **13**, 196.
6 T. A. Seidu, P. T. Kutoka, D. O. Asante, M. A. Farooq, R. N. Alolga and W. Bo, *Pharmaceutics*, 2022, **14**, 1113.
7 B. A. Mukhlif, M. I. Ullah, S. Uthirapathy, S. V. Menon, R. S. Sharma, A. J. Kadhim, S. Sharma, B. Juneja, M. K. Abosaoda and W. R. Kadhum, *J. Radioanal. Nucl. Chem.*, 2025, **334**(2), 1107–1121.
8 S. Islam and R. C. Walker, *Cancer J.*, 2013, **19**, 208–216.
9 G. Bao, S. Mitragotri and S. Tong, *Annu. Rev. Biomed. Eng.*, 2013, **15**, 253–282.
10 M. Woźniak, A. Płoska, A. Siekierzycka, L. W. Dobrucki, L. Kalinowski and I. T. Dobrucki, *Int. J. Mol. Sci.*, 2022, **23**, 2658.
11 Y. Lv, W. Li, W. Liao, H. Jiang, Y. Liu, J. Cao, W. Lu and Y. Feng, *Int. J. Nanomed.*, 2024, **19**, 541–569.
12 S. Hussain, I. Mubeen, N. Ullah, S. S. U. D. Shah, B. A. Khan, M. Zahoor, R. Ullah, F. A. Khan and M. A. Sultan, *BioMed Res. Int.*, 2022, **2022**, 5164970.
13 S. M. Janib, A. S. Moses and J. A. MacKay, *Adv. Drug Delivery Rev.*, 2010, **62**, 1052–1063.
14 F. M. Lu and Z. Yuan, *Quant. Imaging Med. Sur*, 2015, **5**, 433–447.
15 T. Vitor, K. M. Martins, T. M. Ionescu, M. L. D. Cunha, R. H. Baroni, M. R. T. Garcia, J. Wagner, G. C. Neto Campos, S. A. Nogueira, E. G. Guerra and E. Junior Amaro, *Einstein*, 2017, **15**, 115–118.
16 S. Sim and N. K. Wong, *Biomed. Rep.*, 2021, **14**, 42.
17 F. Man, T. Lammers and R. de Rosales, *Mol. Imaging Biol.*, 2018, **20**, 683–695.
18 M. Swierczewska, G. Liu, S. Lee and X. Chen, *Chem. Soc. Rev.*, 2012, **41**, 2641–2655.
19 E. J. van Beek and E. A. Hoffman, *Clin. Chest Med.*, 2008, **29**, 195–216.
20 C. P. Foley, N. Nishimura, K. B. Neeves, C. B. Schaffer and W. L. Olbricht, *Ann. Biomed. Eng.*, 2012, **40**, 292–303.
21 J. J. Vaquero and P. Kinahan, *Annu. Rev. Biomed. Eng.*, 2015, **17**, 385–414.
22 A. Barragán-Montero, U. Javaid, G. Valdés, D. Nguyen, P. Desbordes, B. Macq, S. Willems, L. Vandewinckele, M. Holmström, F. Löfman, S. Michiels, K. Souris, E. Sterpin and J. A. Lee, *Phys. Med.*, 2021, **83**, 242–256.
23 B. Bortot, A. Mangogna, G. Di Lorenzo, G. Stabile, G. Ricci and S. Biffi, *J. Nanobiotechnol.*, 2023, **21**, 155.
24 S. He, S. Chen, D. Li, Y. Wu, X. Zhang, J. Liu, J. Song, L. Liu, J. Qu and Z. Cheng, *Nano Lett.*, 2019, **19**, 2985–2992.
25 C. P. Foley, N. Nishimura, K. B. Neeves, C. B. Schaffer and W. L. Olbricht, *Ann. Biomed. Eng.*, 2012, **40**, 292–303.
26 T. B. Uyar, K. Wu, M. He, I. Khan, M. Royzen and M. V. Yigit, *Chem. Med. Chem.*, 2020, **15**, 988–994.
27 J. RuizdelRio, G. Guedes, D. Novillo, E. Lecue, A. Palanca, A. L. Cortajarena and A. V. Villar, *Theranostics*, 2024, **14**, 176–202.
28 S. Surasinghe, I. Liatsou, Z. Nováková, C. Bařinka, D. Artemov and S. Hapuarachchige, *ACS Appl. Mater. Interfaces*, 2025, **17**, 11611–11623.

29 A. Halim, S. K. Mondal, N. Al-Qadi, E. Kenyon, K. MacRenaris, T. V. O'Halloran, Z. Medarova and A. Moore, *J. Vis. Exp.*, 2024, **210**, e66961.
30 J. Wahsner, E. M. Gale, A. Rodríguez-Rodríguez and P. Caravan, *Chem. Rev.*, 2019, **119**, 957–1057.
31 J. Estelrich, M. J. Sánchez-Martín and M. A. Busquets, *Int. J. Nanomed.*, 2015, **10**, 1727–1741.
32 X. Cheng, Q. Xie and Y. Sun, *Front Bioeng. Biotechnol.*, 2023, **11**, 1177151.
33 S. H. Zhang, W. Xu, P. Gao, W. L. Chen and Q. Zhou, *Artif. Cells Nanomed. Biotechnol.*, 2020, **48**, 169.
34 C. Huang, W. Huang, L. Zhang, C. Zhang, C. Zhou, W. Wei, Y. Li, Q. Zhou, W. Chen and Y. Tang, *Pharmaceutics*, 2022, **14**, 1083.
35 R. Zhang, K. Lu, L. Xiao, X. Hu, W. Cai, L. Liu, Y. Liu, W. Li, H. Zhou, Z. Qian, S. Wang, C. Chen, J. Zeng and M. Gao, *Front Bioeng. Biotechnol.*, 2023, **11**, 1279446.
36 F. Garello, E. Cavallari, M. Capozza, M. Ribodino, R. Parolisi, A. Buffo and E. Terreno, *Magn. Reson. Med.*, 2025, **93**, 761–774.
37 R. Zhang, M. Liu, S. Liu, X. Liang, R. Lu, X. Shuai, D. Wu and Z. Cao, *Acta Biomater.*, 2023, **172**, 454–465.
38 A. A. Chaudhry, S. Naim, M. Gul, A. Chaudhry, M. Chen, R. Jandial and B. Badie, *Radiol. Clin. North Am.*, 2019, **57**, 1189–1198.
39 X. Li, W. Huang and J. H. Holmes, *Magn. Reson. Imaging Clin. N Am.*, 2024, **32**, 47–61.
40 R. L. Gullo, S. C. Partridge, H. J. Shin, S. B. Thakur and K. Pinker, *AJR Am. J. Roentgenol.*, 2024, **222**, e2329933.
41 C. Huang, J. Liang, M. Ma, Q. Cheng, X. Xu, D. Zhang, C. Shi, N. Shang, Z. Xiao and L. Luo, *Front Oncol*, 2020, **10**, 563932.
42 Q. Ma, S. Wu, L. Yang, Y. Wei, C. He, W. Wang, Y. Zhao, Z. Wang, S. Yang, D. Shi, Y. Liu, Z. Zhou, J. Sun and Y. Zhou, *Adv. Sci.*, 2023, **10**, e2202416.
43 J. Cao, H. An, X. Huang, G. Fu, R. Zhuang, L. Zhu, J. Xie and F. Zhang, *Nanoscale*, 2016, **8**, 10152–10159.
44 F. Bruno, V. Granata and F. Cobianchi Bellisari, *Cancers*, 2022, **14**, 1626.
45 S. Gupta, V. Mishra, A. A. Aljabali, A. Albutti, R. Kanday, M. El-Tanani and Y. Mishra, *RSC Adv.*, 2025, **15**, 8019–8052.
46 L. Devkota, R. Bhavane, C. T. Badea, E. A. Tanifum, A. V. Annapragada and K. B. Ghaghada, *Wiley Interdiscip. Rev.:Nanomed. Nanobiotechnol.*, 2025, **17**, e70004.
47 D. Y. Zhang, Y. Zheng, H. Zhang, G. G. Yang, C. P. Tan, L. He, L. N. Ji and Z. W. Mao, *Nanoscale*, 2018, **10**, 22252–22262.
48 P. C. Naha, J. C. Hsu, J. Kim, S. Shah, M. Bouché, S. Si-Mohamed, D. N. Rosario-Berrios, P. Douek, M. Hajfathalian, P. Yasini, S. Singh, M. A. Rosen, M. A. Morgan and D. P. Cormode, *ACS Nano*, 2020, **14**, 10187–10197.
49 J. C. Chow, *Biomolecules*, 2025, **15**, 444.
50 J. C. Chow, *Multimodal Biomedical Imaging Techniques*, 2025, pp. 147–180.
51 P. Paakkari, S. I. Inkinen, J. Jäntti, J. Tuppurainen, M. C. Fugazzola, A. Joenathan, S. Ylisiurua, M. T. Nieminen, H. Kröger, S. Mikkonen, R. van Weeren, B. D. Snyder, J. Töyräs, M. K. M. Honkanen, H. Matikka, M. W. Grinstaff, J. T. J. Honkanen and J. T. A. Mäkelä, *Ann. Biomed. Eng.*, 2025, **53**, 1423–1438.
52 S. Liang, M. Ren, Y. Chen, Z. Song, Y. Yang and H. Zhang, *ACS Omega*, 2025, **10**, 10979–10986.
53 N. Łopuszyńska and W. P. Węglarz, *Nanomaterials*, 2023, **13**, 2163.
54 M. L. Carlson, I. M. Jackson, E. C. Azevedo, S. T. Reyes, I. S. Alam, R. Kellow, J. B. Castillo, S. C. Nagy, R. Sharma, M. Brewer, J. Cleland, B. Shen and M. L. James, *Mol. Imaging Biol.*, 2023, **25**, 1063–1072.
55 Q. Chen, X. Fu, H. Cai, S. Fu, Z. Cai, M. Li, X. Wu, R. Tian and H. Ai, *Regener. Biomater.*, 2023, **10**, rbad029.
56 P. Gouel, P. Decazes, P. Vera, I. Gardin, S. Thureau and P. Bohn, *Front Med*, 2023, **10**, 1055062.
57 A. Polyak and T. L. Ross, *Curr. Med. Chem.*, 2018, **25**, 4328–4353.
58 Z. Cheng, P. Chen and J. Yan, *EJNMMI Phys.*, 2025, **12**, 9.
59 A. Dickhout, P. Van de Vijver, N. Bitsch, S. J. van Hoof, S. L. G. D. Thomassen, S. Massberg, P. Timmerman, F. Verhaegen, R. R. Koenen, I. Dijkgraaf and T. M. Hackeng, *Biomolecules*, 2022, **12**, 829.
60 M. S. O. Pijeira, H. Viltres, J. Kozempel, M. Sakmár, M. Vlk, D. İlem-Özdemir, M. Ekinci, S. Srinivasan, A. R. Rajabzadeh, E. Ricci-Junior, L. M. R. Alencar, M. Al Qahtani and R. Santos-Oliveira, *EJNMMI Radiopharm. Chem.*, 2022, **7**, 8.
61 Y. Yang, J. Wang, Y. Zhong, M. Tian and H. Zhang, *ACS Appl. Mater. Interfaces*, 2025, **17**(3), 4316–4336.
62 V. Bentivoglio, M. Varani, C. Lauri, D. Ranieri and A. Signore, *Biomolecules*, 2022, **12**, 1517.
63 M. B. Cooley, D. Wegierak and A. A. Exner, *Wiley Interdiscip. Rev.:Nanomed. Nanobiotechnol.*, 2024, **16**, e1957.
64 X. Tang, M. Zhao, W. Li and J. Zhao, *Diagnostics*, 2022, **12**, 2582.
65 M. B. Cooley, D. Wegierak, R. Perera, E. Abenojar, P. Nittayacharn, F. M. Berg, Y. Kim, M. C. Kolios and A. A. Exner, *ACS Nano*, 2024, **18**, 33181–33196.
66 S. Wang, J. A. Hossack and A. L. Klibanov, *Invest. Radiol.*, 2020, **55**, 559–572.
67 L. Privitera, I. Paraboschi, D. Dixit, O. J. Arthurs and S. Giuliani, *Innov. Surg. Sci.*, 2022, **6**, 161–172.
68 G. E. Olsson, R. V. Patil, S. J. Chin, K. N. Rus, E. E. Sweeney, K. V. Sharma and R. Fernandes, *Bioeng. Transl. Med.*, 2025, **10**, e10749.
69 M. Ye, J. Zhou, Y. Zhong, J. Xu, J. Hou and X. Wang, *ACS Appl. Mater. Interfaces*, 2019, **11**, 9702–9715.
70 C. L. Nawijn, T. Segers, G. Lajoinie, S. Berg, S. Snipstad, C. de Lange Davies and M. Versluis, *Ultrasound Med. Biol.*, 2024, **50**, 1099–1107.
71 C. Einen, S. Snipstad, H. F. Wesche, V. Nordlund, E. J. Devold, N. Amini, R. Hansen, E. Sulheim and C. de Lange Davies, *J. Control. Release.*, 2025, **378**, 656–670.
72 A. T. Guduru, A. Mansuri, U. Singh, A. Kumar, D. Bhatia and S. V. Dalvi, *Biomater. Adv.*, 2024, **161**, 213886.

73 S. K. Gharat, S. C. Godiyal, P. P. Malusare, K. R. Jadhav and V. J. Kadam, *Curr. Drug Targets*, 2022, **23**, 960–977.
74 M. J. Blomley, J. C. Cooke, E. C. Unger, M. J. Monaghan and D. O. Cosgrove, *BMJ*, 2001, **322**, 1222–1225.
75 M. Sabbaghan, S. Nigam, I. Kasabasic, M. Manepalli, P. Wang and J. Fan, *J. Magn. Reson. Imaging*, 2025, DOI: 10.1002/jmri.29779.
76 R. Zhao, D. Lan, B. Xia, M. Dong, J. Mu and Y. Zhao, *Small*, 2025, 2409713.
77 M. A. Klenner, G. Pascali, M. Massi and B. H. Fraser, *Chem.–Eur. J.*, 2021, **27**, 861–876.
78 R. A. Abdo, F. Lamare, P. Fernandez and M. Bentourkia, *Nucl. Med. Mol. Imaging*, 2021, **55**, 107–115.
79 Y. Tu, X. Ma and H. Chen, *Int. J. Nanomed.*, 2022, **17**, 6773–6789.
80 D. B. Cowan, R. Yao, V. Akurathi, E. R. Snay, J. K. Thedsanamoorthy and D. Zurakowski, *PLoS One*, 2016, **11**, e0160889.
81 S. R. Cherry, *Semin. Nucl. Med.*, 2009, **39**, 348–353.
82 R. Toy, L. Bauer, C. Hoimes, K. B. Ghaghada and E. Karathanasis, *Adv. Drug Delivery Rev.*, 2014, **76**, 79–97.
83 I. J. Lee, J. Y. Park, Y. I. Kim, Y. S. Lee, J. M. Jeong, J. Kim, E. E. Kim, K. W. Kang, D. S. Lee, S. Jeong, E. J. Kim, Y. I. Kim and J. W. Chung, *Mol. Imaging*, 2017, **16**, 1536012116689001.
84 D. G. McGonagle, C. Bridgewood and H. Marzo-Ortega, *Ann. Rheum. Dis.*, 2023, **82**, e164.
85 C. H. Liu and P. Grodzinski, *Radiol. Imaging Cancer.*, 2021, **3**, e200052.
86 S. Shi, F. Chen, S. Goel, S. A. Graves, H. Luo, C. P. Theuer, J. W. Engle and W. Cai, *Nanomicro. Lett.*, 2018, **10**, 65.
87 C. E. O'Hanlon, K. G. Amede, M. R. O'Hear and J. M. Janjic, *J. Fluorine Chem.*, 2012, **137**, 27–33.
88 C. Stigliano, M. R. Ramirez, J. V. Singh, S. Aryal, J. Key, E. Blanco and P. Decuzzi, *Adv. Healthc. Mater.*, 2017, **6**, 1201686.
89 M. Pan, R. Zhao and C. Fu, *Nat. Commun.*, 2024, **15**, 7824.
90 G. Si, S. Hapuarachchige and D. Artemov, *ACS Appl. Nano Mater.*, 2022, **5**, 9625–9632.
91 M. Jeon, M. V. Halbert, Z. R. Stephen and M. Zhang, *Adv. Mater.*, 2021, **33**, 1906539.
92 D. E. J. Waddington, T. Boele, R. Maschmeyer, Z. Kuncic and M. S. Rosen, *Sci. Adv.*, 2020, **6**, eabb0998.
93 B. Liu, J. Liao, Y. Song, C. Chen, L. Ding, J. Lu, J. Zhou and F. Wang, *Nanoscale Adv.*, 2022, **4**(1), 30–38.
94 T. Ochi, H. Nishiofuku and T. Kure, *Biochem. Biophys. Rep.*, 2023, **34**, 1473.
95 J. Lai, Z. Luo, L. Chen and Z. Wu, *Sci. Prog.*, 2024, **107**, 368504241228076.
96 Z. Jiang, M. Zhang, P. Li, Y. Wang and Q. Fu, *Theranostics*, 2023, **13**, 483–509.
97 D. Wegierak, P. Nittayacharn, M. B. Cooley, F. M. Berg, T. Kosmides, D. Durig, M. C. Kolios and A. A. Exner, *Wiley Interdiscip. Rev.:Nanomed. Nanobiotechnol.*, 2024, **16**, e2007.
98 C. L. Bayer, S. Y. Nam, Y. S. Chen and S. Y. Emelianov, *J. Biomed. Opt.*, 2013, **18**, 16001.
99 G. A. Pang, C. Haisch and J. Laufer, *Nanoscale Adv.*, 2020, **2**, 2699–2704.
100 M. Xu, Z. Chen, J. Zheng, Q. Zhao and Z. Yuan, *Semin. Cancer Biol.*, 2023, **94**, 62–80.
101 J. Rodrigues, A. Amin, S. Chandra, N. J. Mulla, G. S. Nayak, S. Rai, S. Ray and K. K. Mahato, *ACS Sens.*, 2024, **9**, 589–601.
102 T. Yang, Y. Luo, W. Ji and G. Yang, *Biophys. Rep.*, 2021, **7**, 253–266.
103 R. K. Hartman, K. A. Hallam, E. M. Donnelly and S. Y. Emelianov, *Laser Phys. Lett.*, 2019, **16**, 025603.
104 S. Panja, M. Sharma, H. Sharma, A. Kumar, V. Chandel, S. Roy and D. Biswas, *Discover Nano*, 2024, **19**, 214.
105 P. M. Neelamraju, K. Gundepudi, P. K. Sanki, K. B. Busi, T. K. Mistri, S. Sangaraju, G. K. Dalapati, K. K. Ghosh, S. Ghosh, W. B. Ball and S. Chakrabortty, *Heliyon*, 2024, **10**(15), e34654.
106 J. Chen, S. Zeng, Q. Xue, Y. Hong, L. Liu, L. Song, C. Fang, H. Zhang, B. Wang, A. C. Sedgwick, P. Zhang, J. L. Sessler, C. Liu and J. Chen, *Proc. Natl. Acad. Sci. U. S. A.*, 2022, **119**, e2213373119.
107 K. P. Kubelick, J. Kim, M. Kim, X. Huang, C. Wang, S. Song, Y. Xia and S. Y. Emelianov, *ACS Nano*, 2025, **19**, 6079–6094.
108 Y. Sun, P. Zhang, Y. Li, Y. Hou, C. Yin, Z. Wang, Z. Liao, X. Fu, M. Li, C. Fan, D. Sun and L. Cheng, *ACS Nano*, 2022, **16**, 18667–18681.
109 H. Xu, P. She, Z. Zhao, B. Ma, G. Li and Y. Wang, *Adv. Mater.*, 2023, **35**, e2300439.
110 L. Qi, S. Liu, J. Ping, X. Yao, L. Chen, D. Yang, Y. Liu, C. Wang, Y. Xiao, L. Qi and Y. Jiang, *Biosensors*, 2024, **14**, 314.
111 W. Li, G. S. Kaminski Schierle, B. Lei, Y. Liu and C. F. Kaminski, *Chem. Rev.*, 2022, **122**, 12495–12543.
112 T. Andrian, Y. Muela, L. Delgado, L. Albertazzi and S. Pujals, *Nanoscale*, 2023, **15**, 14615–14627.
113 D. Maji, J. Lu, P. Sarder, A. H. Schmieder, G. Cui, X. Yang, D. Pan, M. D. Lew, S. Achilefu and G. M. Lanza, *Precis. Nanomed.*, 2018, **1**, 128–145.
114 Q. Chen, H. Fang, X. Shao, Z. Tian, S. Geng and Y. Zhang, *Nat. Commun.*, 2020, **11**, 6290.
115 V. Romeo, L. Moy and K. Pinker, *PET Clin.*, 2023, **18**, 567–575.
116 P. Alongi, A. Arnone, V. Vultaggio, A. Fraternali, A. Versari, C. Casali, G. Arnone, F. DiMeco and I. G. Vetrano, *Cancers*, 2024, **16**, 407.
117 W. C. Chou, Q. Chen, L. Yuan, Y. H. Cheng, C. He, N. A. Monteiro-Riviere, J. E. Riviere and Z. Lin, *J. Control Release.*, 2023, **361**, 53–63.
118 L. Yang, Q. Liu, P. Kumar, A. Sengupta, A. Farnoud, R. Shen, D. Trofimova, S. Ziegler, N. Davoudi, A. Doryab, A. Ö. Yildirim, M. E. Diefenbacher, H. B. Schiller, D. Razansky, M. Piraud, G. Burgstaller, W. G. Kreyling, F. Isensee, M. Rehberg, T. Stoeger and O. Schmid, *Nat. Commun.*, 2024, **15**, 10138.
119 H. Liu, H. Gao and F. Jia, *Contrast Media Mol. Imaging*, 2021, **2021**, 9032017.
120 D. Jerez, E. Stuart, K. Schmitt, D. Guerrero-Given, J. M. Christie and W. E. Hahn, *Sci. Rep.*, 2021, **11**, 7771.

121 B. R. Kingston, A. M. Syed, J. Ngai, S. Sindhwani and W. C. W. Chan, *Proc. Natl. Acad. Sci. U. S. A.*, 2019, **116**, 14937–14946.
122 L. E. Jennings and N. J. Long, *Chem. Commun.*, 2009, 3511–3524.
123 M. Moseley and G. Donnan, *Stroke*, 2004, **35**, 2632–2634.
124 M. V. Novoselova, S. V. German, T. O. Abakumova, S. V. Perevoschikov, O. V. Sergeeva, M. V. Nesterchuk, O. I. Efimova, K. S. Petrov, V. S. Chernyshev, T. S. Zatsepin and D. A. Gorin, *Colloids Surf., B*, 2021, **200**, 111576.
125 Y. Guo, X. Y. Wang, Y. L. Chen, F. Q. Liu, M. X. Tan, M. Ao, J. H. Yu, H. T. Ran and Z. X. Wang, *Acta Biomater.*, 2018, **80**, 308–326.
126 L. Wen, L. Xia, X. Guo, H. F. Huang, F. Wang, X. T. Yang, Z. Yang and H. Zhu, *Front Oncol*, 2021, **11**, 778728.
127 A. Setia, A. K. Mehata, V. Priya, D. M. Pawde, D. Jain, S. K. Mahto and M. S. Muthu, *Mol. Pharm.*, 2023, **20**, 4922–4941.
128 N. Manners, V. Priya, A. K. Mehata, M. Rawat, S. Mohan, H. A. Makeen, M. Albratty, A. Albarrati, A. M. Meraya and M. S. Muthu, *Pharmaceuticals*, 2022, **15**, 441.
129 X. Chen, Y. Zhang, H. Zhang, L. Zhang, L. Liu, Y. Cao, H. Ran and J. Tian, *J. Nanobiotechnol.*, 2021, **19**, 1–8.
130 S. Shang, Z. Chen, Y. Zhao, S. Yang and D. Xing, *Opt. Express*, 2017, **25**, 530–539.
131 M. Yao, X. Shi, C. Zuo, M. Ma, L. Zhang and H. Zhang, *ACS Appl. Mater. Interfaces*, 2021, **12**, 37885–37895.
132 Y. Liu, Y. Yang, M. Sun, M. Cui, Y. Fu and Y. Lin, *Chem. Sci.*, 2017, **8**, 2710–2716.
133 J. C. Hsu, L. M. Nieves, O. Betzer, T. Sadan, P. B. Noël, R. Popovtzer and D. P. Cormode, *Wiley Interdiscip. Rev.:Nanomed. Nanobiotechnol.*, 2020, **12**, e1642.
134 A. Volpe, E. Kurtys and G. O. Fruhwirth, *Int. J. Biochem. Cell Biol.*, 2018, **102**, 40–50.
135 J. J. J. Tjalma, *Gut*, 2020, **69**, 406–410.
136 M. Andreana, R. Sentosa, M. T. Erkkilä, W. Drexler and A. Unterhuber, *Photochem. Photobiol. Sci.*, 2019, **18**, 997–1008.
137 R. T. Megens, *J. Vasc. Res.*, 2007, **44**, 87–98.
138 C. Chirizzi, *J. Am. Chem. Soc.*, 2021, **143**, 12253–12260.
139 M. L. Scarpelli, D. R. Healey, S. Mehta, V. D. Kodibagkar and C. C. Quarles, *Sci. Rep.*, 2020, **10**, 17324.
140 L. M. Zopf, *Mol. Imaging Biol.*, 2021, **23**, 894.
141 Q. Zhao, N. Cheng, X. Sun, L. Yan and W. Li, *Front Bioeng. Biotechnol.*, 2023, **11**, 1219054.
142 J. Starekova, A. Pirasteh and S. B. Reeder, *Am. J. Roentgenol.*, 2024, **223**, e2330036.
143 N. Levy, *Int. J. Stroke*, 2012, **7**, 440–442.
144 S. Waite, J. Scott and D. Colombo, *Radiology*, 2021, **299**, 27–35.
145 C. Comanescu, *Chemistry*, 2022, **4**, 872–930.
146 N. Yadav, S. Pandey, A. Gupta, P. Dudani, S. Gupta and K. Rangarajan, *Indian Dermatol. Online J.*, 2023, **14**, 788–792.
147 C. Mennella, U. Maniscalco, G. De Pietro and M. Esposito, *Heliyon*, 2024, **10**, e26297.